

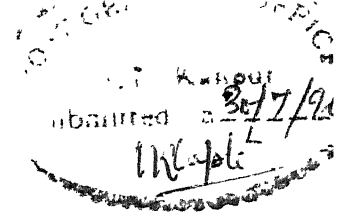
**EXPERIMENTAL PROCEDURE FOR  
DETERMINATION OF  $Q_U$ ,  $Q_{EXT}$ ,  $Q_L$  AND  
COUPLING ( $\beta$ ) OF DIELECTRIC RESONATOR  
(DR) AND DEVELOPMENT OF DR  
OSCILLATOR**

*A Thesis Submitted*  
in Partial Fulfillment of the Requirements  
for the Degree of  
Master of Technology

*by*  
Pavan Kumar

*to the*  
**DEPARTMENT OF ELECTRICAL ENGINEERING  
INDIAN INSTITUTE OF TECHNOLOGY, KANPUR**

# Certificate



It is certified that the work contained in the thesis entitled **EXPERIMENTAL**  
**PROCEDURE FOR DETERMINATION**<sup>OF</sup> <sub>$Q_U$ ,  $Q_{EXT}$ ,  $Q_L$</sub>  **AND COUPLING**  
**( $\beta$ ) OF DIELECTRIC RESONATOR (DR) AND DEVELOPMENT OF**  
**DR OSCILLATOR**, by Pavan Kumar , has been carried out under my supervision  
and that this work has not been submitted elsewhere for a degree.

25 July 1996

  
Dr. A. Biswas

Assistant Professor

Department of Electrical Engineering

I.I.T. Kanpur

14 OCT 1996  
CENTRAL LIBRARY  
I I T., KANPUR  
Inv. No. A. 122312



A122312

EE-1996-M-KUM-EXP

# Abstract

An analytical formulation for determination of Q-factor of dielectric resonator (DR) placed in suspended substrate environment has been presented. Frequency dependent conductor and dielectric losses in the different regions have been calculated to determine the unloaded Q-factor ( $Q_u$ ).

Experimental procedure to measures the coupling between DR and microstrip ( $\beta$ ), has also been presented. An experiment has been performed using HP8410 network analyser and  $\beta$ ,  $Q_{ext}$ ,  $Q_L$ ,  $Q_u$  has been measured to evaluate equivalent circuit parameters of DR. Finally, DR oscillator has been designed and fabricated.

# Abstract

An analytical formulation for determination of Q-factor of dielectric resonator (DR) placed in suspended substrate environment has been presented. Frequency dependent conductor and dielectric losses in the different regions have been calculated to determine the unloaded Q-factor ( $Q_u$ ).

Experimental procedure to measures the coupling between DR and microstrip ( $\beta$ ) has also been presented. An experiment has been performed using HP8410 network analyser and  $\beta$ ,  $Q_{ext}$ ,  $Q_L$ ,  $Q_u$  has been measured to evaluate equivalent circuit parameters of DR. Finally, DR oscillator has been designed and fabricated.

## Acknowledgement

The name of Dr. Animesh Biswas, my thesis guide, came foremost in my mind when I sat down to write this acknowledgement. It would not be exaggerating if I mention that "His guidance was wholesome in itself ". I have tried my best to crystalize his ideas on dielectric resonator oscillators in my M. Tech. thesis.

Also, the inspiring lectures of Dr. Biswas and Prof. M. Sachidananda instilled in me a sense of appreciation and wonder for electromagnetics and microwaves.

I wish to thank my batchmates J. Kumar, Patni, Yash, Manish, Ashish, Jaipal, Jayesh, Sanjay, Raju, Subbu and friends Roopam, Maj. Chow, P. K. Paliwal, Maj. Sehgal and Santosh who have always stood by me during my stay in this campus.

I owe to my family a debt for their numerous sacrifices and moral support. I conclude this acknowledgement with my thanks to them.

## Acknowledgement

The name of Dr. Animesh Biswas, my thesis guide, came foremost in my mind when I sat down to write this acknowledgement. It would not be exaggerating if I mention that "His guidance was wholesome in itself ". I have tried my best to crystalize his ideas on dielectric resonator oscillators in my M. Tech. thesis.

Also, the inspiring lectures of Dr. Biswas and Prof. M. Sachidananda instilled in me a sense of appreciation and wonder for electromagnetics and microwaves.

I wish to thank my batchmates J. Kumar, Patni, Yash, Manish, Ashish, Jaipal, Jayesh, Sanjay, Raju, Subbu and friends Roopam, Maj. Chow, P. K. Paliwal, Maj. Sehgal and Santosh who have always stood by me during my stay in this campus.

I owe to my family a debt for their numerous sacrifices and moral support. I conclude this acknowledgement with my thanks to them.

# Contents

<b>1</b>	<b>INTRODUCTION</b>	<b>1</b>
1.1	DIELECTRIC RESONATOR . . . . .	2
1.1.1	Quality Factor . . . . .	2
1.1.2	Temperature coefficient( $T_f$ ) . . . . .	3
1.1.3	Permittivity ( $\epsilon_r$ ) . . . . .	4
1.2	Measurement of coupling and Q-factor . . . . .	4
1.3	Oscillator . . . . .	6
1.4	Organization of Thesis . . . . .	7
<b>2</b>	<b>Determination of Conductor Losses and Unloaded Q-factor</b>	<b>8</b>
2.1	Defination of Q-factor . . . . .	8
2.2	Determination of Conductor Loss . . . . .	9
2.2.1	Losses in the top plate . . . . .	10
2.2.2	Losses in the bottom ground plate . . . . .	11
2.3	Determination of Unloaded Q-Factor . . . . .	11
2.3.1	Conductor Quality Factor ( $Q_c$ ) . . . . .	11
2.3.2	Q-factor Due to Dielectric Loss . . . . .	12
2.3.3	Overall unloaded Q-factor . . . . .	14



2.4.3	Effect of Substrates Parameter on $Q_u$ . . . . .	17
2.4.4	Effect of DR's Parameter on $Q_u$ . . . . .	19
<b>3</b>	<b>Measurement Procedure for Determination of Coupling (<math>\beta</math>), <math>Q_u</math>, <math>Q_{ext}</math> and <math>Q_L</math></b>	<b>22</b>
3.1	Circuit Parameters: An Introduction . . . . .	22
3.2	Coupling Factor of DR Coupled to Microstrip . . . . .	24
3.3	Measurement Setup . . . . .	27
3.4	Calculation for $\beta$ , $Q_L$ , $Q_u$ and $Q_{ext}$ . . . . .	29
3.5	Results . . . . .	35
<b>4</b>	<b>Design and Fabrication of DR Oscillator</b>	<b>37</b>
4.1	Theory of Oscillation . . . . .	37
4.2	Oscillator Design . . . . .	39
4.3	Choice of transistor and its biasing . . . . .	40
4.3.1	Choice of transistor . . . . .	40
4.3.2	Biasing of the transistor . . . . .	41
4.4	Stability Consideration . . . . .	42
4.4.1	Calculation of S-parameter with feedback capacitor . . . . .	43
4.4.2	Design of open circuit stub to obtain capacitance at source terminals . . . . .	44
4.5	Input and Output Matching Network . . . . .	44
4.5.1	Design of Output Matching Network . . . . .	45
4.5.2	Design of Input Matching Network . . . . .	45
<b>5</b>	<b>Conclusion and suggestion for future Development</b>	<b>48</b>

# List of Figures

1.1	Different Shape of Dielectric Resonator . . . . .	2
1.2	DR Coupled to a Microstrip Line . . . . .	5
1.3	Equivalent Circuit of Fig1.2 . . . . .	5
2.1	Cross sectional view of DR placed in SS environment . . . . .	9
2.2	DR in Shielded Environment . . . . .	15
2.3	Unloaded Q-factor of DR placed in MIC environment . . . . .	15
2.4	Conductor Q-factor of in SS Environment . . . . .	17
2.5	Unloaded and dielectric loss Q-factor of in SS Environment . . . . .	18
2.6	Effect of substrate thickness on Unloaded Q-factor of in SS Environment	18
2.7	Effect of $\epsilon_{ds1}$ on $Q_u$ . . . . .	19
2.8	Effect of radius of DR on $Q_u$ . . . . .	20
2.9	Effect of Thickness of DR on $Q_u$ . . . . .	20
2.10	Effect of $\epsilon_r$ of DR on $Q_u$ . . . . .	21
3.1	Low frequency resonant circuit . . . . .	23
3.2	Coupling between DR and Microstrip . . . . .	25
3.3	Equivalent circuit of DR coupled to microstrip . . . . .	26
3.4	Experimental setup . . . . .	28
3.5	Measured $S_{11}$ for different spacing 'y' . . . . .	28
3.6	Measured $S_{12}$ for different spacing 'y' . . . . .	29

3.8	Measured $S_{12}$ around resonance for different spacing 'y' . . . . .	30
3.9	Coupling between DR and microstrip . . . . .	31
3.10	Definition of various terms in reflection plane . . . . .	32
3.11	Definition of various terms in transmission plane . . . . .	32
3.12	Variation of $Q_L$ and $Q_{ext}$ of Loaded DR . . . . .	33
3.13	Equivalent resistance of DR coupled to microstrip . . . . .	34
3.14	Equivalent inductance of DR coupled to microstrip . . . . .	35
3.15	Equivalent capacitance of DR coupled to microstrip . . . . .	36
4.1	Block diagram of an oscillator [17] . . . . .	38
4.2	Oscillation in port 1 [17] . . . . .	39
4.3	DR as a series feedback element in DRO [16] . . . . .	40
4.4	Device characteristic . . . . .	41
4.5	circuit diagram of oscillator [18] . . . . .	42
4.6	Equivalent Circuit of Oscillator [17] . . . . .	45
4.7	PCB layout of the oscillator circuit . . . . .	46

# List of Tables

1.1	Material composition and composition of few DR materials . . . . .	4
2.1	Comparison of present theoretical data for $Q_u$ with that of reported data . . . . .	16
3.1	Data for coupling and unloaded Q-factor of DR coupled with microstrip	34
4.1	Data for width and effective dielectric constant of microstrip . . . . .	46

# Chapter 1

## INTRODUCTION

Microwave systems like radar, electronic warfare, navigation, surveillance and weapon guidance system are largely military in nature and research in these fields have been largely sustained by defense community throughout the globe. Microwave are also used in commercial systems like cellular phone, microwave oven, data communications and video/audio communications.

Now a days, reduction in the cost and size are main the parameters in the design consideration of microwave circuits. Although bulky waveguide and rigid coaxial lines are replaced by microstrip and striplines but former are still used in some application, such as high power transmissions line or low loss filters. In the design of microwave systems like filter, mixer and oscillator, a frequency determining element is required. Metal cavity resonator, SAW (Surface Acoustic Wave) or microstrip line can be used as frequency determining element. With the advent of high dielectric constant, temperature stable and low loss material, Dielectric Resonator(DR) can also be used for same purpose. DRs are compatible to microstrip and suspended stripline for design of microwave circuits. The size of DR is considerably smaller ( $1/\sqrt{\epsilon_r}$ ) than the size of empty metal cavity operating at same frequency. They are

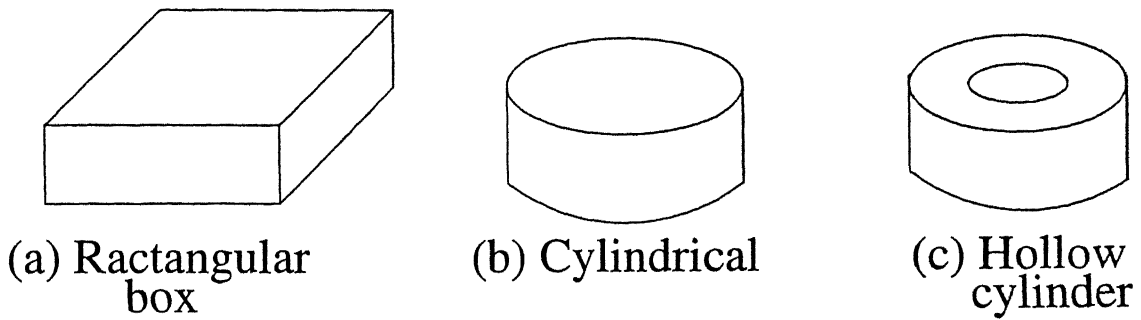


Figure 1.1: Different Shape of Dielectric Resonator

## 1.1 DIELECTRIC RESONATOR

R.D.Richtmayer in 1939 observed that unmetallized dielectric objects can function as dielectric resonators. Its resonant frequency, modes, and circuit properties were first verified experimentally in 1960.

DRs are made of low-loss, temperature stable, high permittivity and high  $Q$  ceramic material in a regular geometrical form. The shape of DR is usually a short and solid cylinder but one can also find tabular, spherical and paralleled as shown in figure 1.1. A commonly used resonant mode in cylindrical DRs is  $TE_{01\delta}$ . This shape of DR is preferred over other shapes because this does not have a large number of degenerative modes and is easier to fabricate and mount in microwave circuits. Its resonant frequency is determined by its dimensions and shielding condition. Because of its small size, low price and excellent integrability in MICs, it is very useful in both active and passive circuits.

### 1.1.1 Quality Factor

Quality factor of a circuit is a very important parameter because it limits the overall performance of the circuit. Higher value of  $Q$  is required in design of oscillators.

The unloaded quality factor of DR placed in suspended substrate environment depends upon loss in the DRs material, conductor loss of the shielding wall and

past to compute the Q-factor [1]-[4]. Although these methods are quite accurate but are highly numerical in nature. Kajfež [5] has described method of perturbation for computing Q-factor for DR in MIC environment. This determines the Q-factor indirectly by computing the relative change in resonant frequency when the conducting walls of the DR structure are moved inwards by an amount equal to skin depth. Although this method is quite accurate but lot of caution may be required when applying this method, because these two frequencies (perturbed and unperturbed) are very close to each other.

In this thesis Q-factor is determined for generalized two layer substrate by computing the stored energy and power loss. This method is approximate but quite accurate and data calculated by this method can be used in design purposes. Mongia [6] has done same work for MIC environment, but he did not incorporated frequency dependent dielectric loss in DRs and substrates. These losses might be significant at higher frequency.

### 1.1.2 Temperature coefficient( $T_f$ )

The temperature coefficient ( $T_f$ ) of a DR can be controlled by modifying the composition, to be anywhere with in +9 to -9 p.p.m/ $^{\circ}$ c. Change in any circuit parameter can also shifts  $T_f$  by few part per million.

Table 1.1 [7] shows the properties of certain material used in DR.

In table 1.1 no composition have overall superiority over the others, since many factor, such as ease of ceramic processing and ability to hold tolerances on the dielectric properties must be considered.

Material composition	$Q_0$	$\epsilon_r$	Freq range (GHz.)	Temp coeff. ( $T_f$ (ppm/°c))
(ZrSn)Ti oxide	10,000(4.5GHz.)	35.7-36.4	1.45-8.86	-3 to +9
BaLnTi oxide	3,000(3 GHz.)	80.0	0.7-3.62	-3 to +9
BaZnTaTi oxide	10,000(10GHz.)	27.6-30.6	5.5-32.2	-4 to +4
Ba Titaniam oxide	6,000(4.5GHz.)	36.6-38.3	0.8-5.21	0 to 4

Table 1.1: Material composition and composition of few DR materials

### 1.1.3 Permittivity ( $\epsilon_r$ )

As shown in the table1.1  $\epsilon_r$  of DR is in the range between 29 to 80. For low dielectric constant materials performance is likely to be more sensitive to shielding due to increase of field outside the resonator. When  $\epsilon_r$  is around 40 more than 95% of stored electric energy as well as 60% of the stored magnetic energy are located within the resonator for  $TE_{01\delta}$  mode.

## 1.2 Measurement of coupling and Q-factor

The complete characterization of microstrip line coupled with DR, as shown in figure1.2 and figure1.3, is necessary for the analysis and synthesis of integrated circuits. Ginzton [8] introduced the plotting of loci of various Q-factors. Podcameni [9] suggested a relation for determination of unloaded Q of DR using an indirect method. A simple method is presented in [10] to measure the coupling ( $\beta$ ),  $Q_u$ ,  $Q_{ex}$  and  $Q_L$  in terms of directly measurable quantities in both reflection and transmission coefficient plane. They also draw the loci for different coupling on smith chart.

However, in this thesis these quantities have been directly measured from the plots of reflection coeff. and transmission coeff. with respect to frequency. This



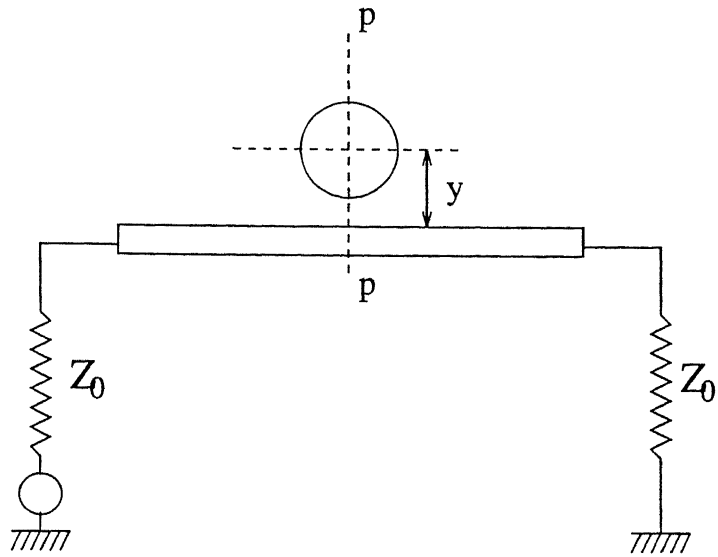


Figure 1.2: DR Coupled to a Microstrip Line

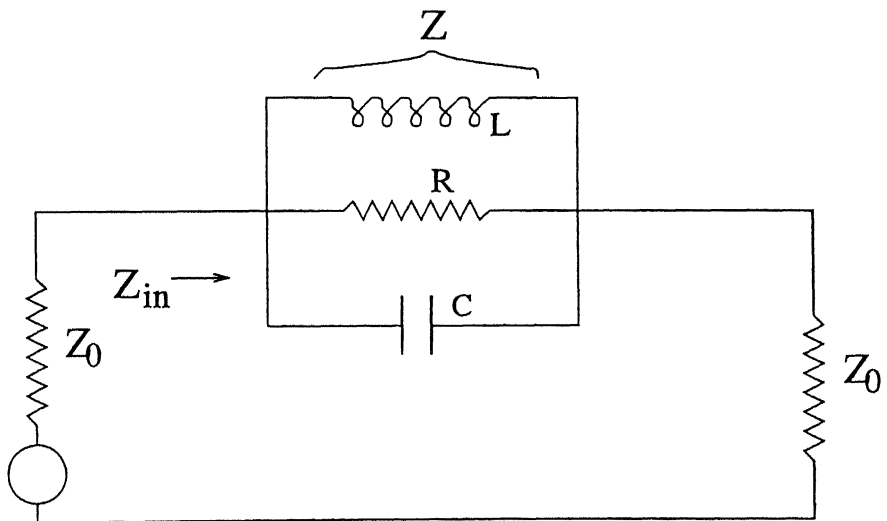


Figure 1.3: Equivalent Circuit of Fig1.2

## 1.3 Oscillator

Oscillators represent the basic microwave energy source for all microwave systems such as radars, communication, navigation, and electronic warfare. They can be termed as D.C to R.F converter or an infinite gain amplifier. Typical microwave oscillator essentially have an active device (BJT or FET) and a passive frequency determining element such as a microstrip, SAW, cavity resonator or DR for fixed frequency oscillation and YIG (Yttrium Iron Garnet) sphere for tunable oscillator. Microwave oscillator using GUNN or IMPATT diodes dates back to the late 1960s, before that magnetron and klystron were used as sources. Magnetron and klystron are still used for high power application.

Quartz crystal oscillators represent highly stable source, but their operation is limited to few mega Hertz. At microwave frequency these are realised using frequency multiplication. In this process power is increased but at the cost of higher noise figure and less efficiency of device.

With the development of B.J.T and of GaAs MESFET devices at microwave frequency, now transistor based oscillator can be realised at such frequencies. Bipolar oscillator have maximum oscillation frequency which is lower than that of GaAs FET oscillator but later is noiser than the former.

Present trend of oscillator design is mostly emphasised low noise, small size, light weight, high efficiency, temperature stable, low cost and reliable for all fixed frequency oscillation. Tunable oscillator should additionally have wider band-width, better tuning linearity and reduced settling time.

In this thesis, oscillators are designed using DR as the passive element. Due to its high Q, small size, and excellent integrability in suspended substrate and MIC environment it can be directly used as frequency determining element for realising stable transistor oscillator. Because of its special properties, the transistor dielectric

## 1.4 Organization of Thesis

The thesis has been divided in five chapters. Chapter 1 is introduction which deals with previous work in this area and procedures used in other chapters of this thesis. Chapter 2 deals with the determination of unloaded quality factor. In chapter 3 experimental procedure have been discussed for measurement of coupling and various Q factors. Chapter 4 discusses the design procedure of oscillator with DR as passive and FET as active element. In the last chapter results and future development have been discussed.

# Chapter 2

## Determination of Conductor Losses and Unloaded Q-factor

The intrinsic Q-factor of a dielectric resonator, which is determined by the dielectric losses of resonator material, is usually very high. When a DR is shielded by conducting walls in the practical circuits, the unloaded Q-factor of the resonator is degraded due to conductor loss in the top and bottom shielding walls and the dielectric loss in the substrate. Mode matching technique used for analysis of  $TE_{01\delta}$  mode for the structure shown in figure 2.1, has been given in [11]. The field expression calculated using this technique have been used to compute the conductor losses and conductor Q-factor( $Q_c$ ).

### 2.1 Defination of Q-factor

The Q-factor is assurance of the performance or quality of resonator, is measure of energy loss or dissipation loss per cycle as compared to the stored energy. Q-factor is defined by

$$Q = 2\pi \frac{\text{max. stored energy}}{\text{energy dissipated per cycle}}$$

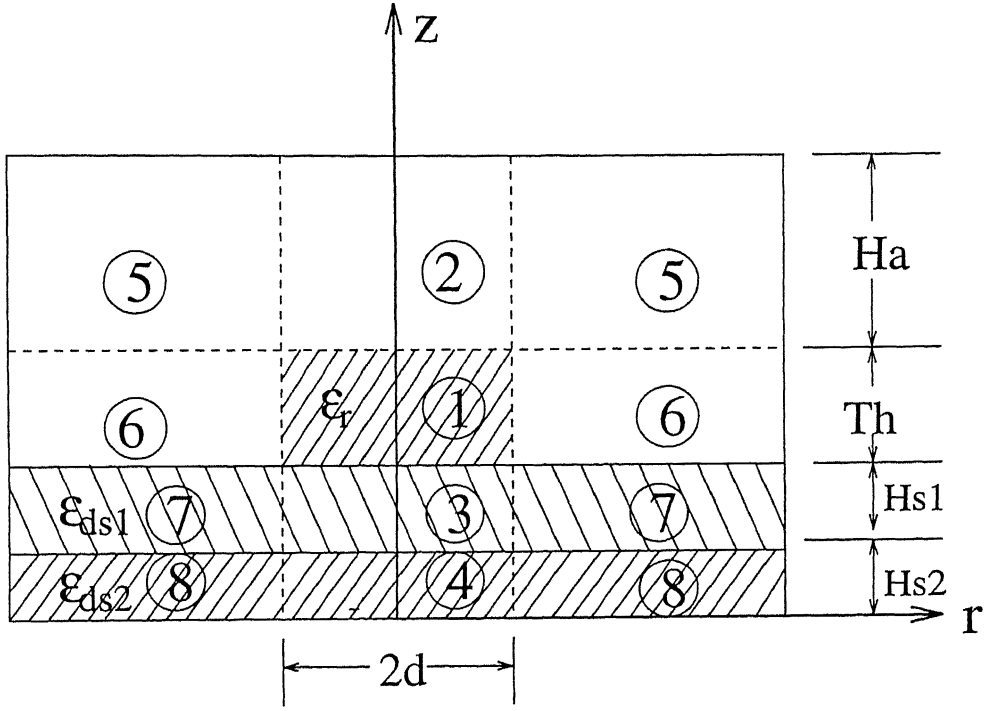


Figure 2.1: Cross sectional view of DR placed in SS environment

Let  $W_e$  and  $W_m$  are the stored electric and magnetic energy respectively,  $f_0$  is the resonant frequency and  $P_c$  is total loss, then  $Q$  will be given by

$$Q = 2\pi \frac{(W_e + W_m)}{P_c/f_0} \quad (2.1)$$

EDC (effective dielectric constant) method has been used to evaluate resonant frequency ( $f_0$ ) of DR in suspended substrate environment [12]. This method requires range in which  $f_0$  lies. Formula to determine lower limit of this range is given in [12], while the upper limit needs to be provided for each set of data. We incorporate a formula for this upper limit.

## 2.2 Determination of Conductor Loss

then the conductor loss  $P_c$  can be expressed as

$$P_c = \frac{1}{2} R_m \int |J_c|^2 ds \quad (2.2)$$

Where  $R_m$  is real part of surface impedance and given by

$$R_m = \sqrt{\pi f_0 \mu_0 / \sigma} \quad (2.3)$$

Where  $\sigma$  is conductivity of top and bottom ground plate.

### 2.2.1 Losses in the top plate

In the design of microwave systems containing a DR, generally the top ground plate is much away than the bottom ground plane from DR. So the loss in this plate has lesser effect on overall unloaded Q-factor. Mathematically this loss are represented by

$$P_{c(top)} = \frac{1}{2} R_m \int |J_c|^2 ds \quad (2.4)$$

The surface current  $J_c$  can be calculated from the boundary condition  $J_c = \hat{n} \times \hat{H}$ , where  $\hat{n}$  is the unit normal vector of the surface. From figure 2.1, it is clear that  $\hat{n} = \hat{z}$ . Since  $H_r$ ,  $H_z$  and  $E_\phi$  component of fields will be exist for  $TE_{01\delta}$  (where  $\delta$  is slightly less than one) mode in DR, surface current  $J_c$  will be contributed only due to  $H_r$ . Hence,  $J_c = \hat{z} \times H_r$  (region 2 and 5) and from Maxwell's equation  $H_r$  is given by

$$H_r = \frac{1}{k_r^2} \frac{\partial^2 H_z}{\partial r \partial z} \quad (2.5)$$

Finally, after satisfying the value of  $J_c$  in equation 2.4 we get the expression for  $P_{c(top)}$  as follows.

$$P_{c(top)} = \pi R_m \alpha_a^2 B_2^2 \cdot \exp(-2\alpha_a d_1) \left[ \frac{I_1}{k_r^2} + \frac{I_2 B_7^2}{k_a^2} \right] \quad (2.6)$$

Where  $B_i$ 's,  $k_r$  and  $k_a$  are the amplitude, radial wave number and axial wave numbers

## 2.2.2 Losses in the bottom ground plate

Loss in the bottom ground plate play the dominant role in the calculation of unloaded Q-factor. Mathematically this is given by

$$P_{c(bottom)} = \frac{1}{2} R_m \int |J_{c(bottom)}|^2 ds \quad (2.7)$$

$$J_{c(bottom)} = \hat{z} \times \hat{H}_r(region4, 8)$$

and  $H_r$  is given by

$$H_r = \frac{1}{k_a^2} \frac{\partial^2 H_z}{\partial r \partial z} \quad (2.8)$$

The final expression of  $P_{c(bottom)}$  is given by

$$P_{c(bottom)} = \pi R_m \alpha_s^2 B_5^2 \cdot \exp(-2\alpha_s d_2) \left[ \frac{I_1}{k_r^2} + \frac{I_2 B_7^2}{k_a^2} \right] \quad (2.9)$$

Where  $\alpha_a$  and  $\alpha_s$  are the constants and are given in [11].

## 2.3 Determination of Unloaded Q-Factor

### 2.3.1 Conductor Quality Factor ( $Q_c$ )

With continued progress in the development of DR material, the conductor loss and dielectric loss in the substrate become important factors in determination of overall unloaded Q-factor. Conductor Q-factor is determined using equation 2.1. Expressions for total electric and magnetic energies inside the structure having the DR are given by

$$W_e = \sum_{i=1}^8 \frac{1}{4} \epsilon_0 \epsilon_r \int |E_{\phi_i}|^2 dv = \sum_{i=1}^8 W_{e_i} \quad (2.10)$$

$$W_m = \sum_{i=1}^8 \frac{1}{4} \mu_0 \mu_r \int |H_{\phi_i}|^2 dv = \sum_{i=1}^8 W_{m_i} \quad (2.11)$$

Where 'i' is the region number.

including DR will be same at a resonant frequency. So complete structure is needed for determination of electric energy required for calculation of  $Q_c$ . Which is given by

$$Q_{c(top)} = \frac{2\pi f_0(W_e + W_m)}{P_{c(top)}} \quad (2.12)$$

$$Q_{c(bottom)} = \frac{2\pi f_0(W_e + W_m)}{P_{c(bottom)}} \quad (2.13)$$

Total conductor losses,  $P_c$ , are given by

$$\Rightarrow P_c = P_{c(top)} + P_{c(bottom)} \quad (2.14)$$

$$\Rightarrow \frac{P_c}{2\pi f_0(W_e + W_m)} = \frac{P_{c(top)}}{2\pi f_0(W_e + W_m)} + \frac{P_{c(bottom)}}{2\pi f_0(W_e + W_m)} \quad (2.15)$$

$$\Rightarrow \frac{1}{Q_c} = \frac{1}{Q_{c(top)}} + \frac{1}{Q_{c(bottom)}} \quad (2.16)$$

$$(2.17)$$

### 2.3.2 Q-factor Due to Dielectric Loss

Intrinsic Q-factor of the DR ( $Q_{dr}$ ) is dependent upon on loss tangent of DR materials.  $Q_d$  of DR in the suspended substrate environment or MIC environment does not exactly equals  $1/\tan\delta$ . It also depends upon electric energy distribution inside and outside the resonator. A similar argument, is applicable to Q-factor due to dielectric loss in the substrate. By defination  $Q_d$  is given by;

$$Q_d = \omega \frac{W}{P_d} \quad (2.18)$$

Where  $W = W_e + W_m$  and  $P_d = 2\omega W_d \tan\delta$

Hence Q-factor due to dielectric loss in different regions are

- Q-factor due to resonator loss is



- Q-factor due to substrate1 (region3 and 7) is

$$Q_{ds1} = \frac{W_e}{(W_{e3} + W_{e7})} \frac{1}{\tan\delta_{ds1}} \quad (2.20)$$

- Q-factor due to substrate1 (region4 and 8) is

$$Q_{ds2} = \frac{W_e}{(W_{e4} + W_{e8})} \frac{1}{\tan\delta_{ds2}} \quad (2.21)$$

Here,  $\tan\delta_{dr}$  and  $\tan\delta_{ds1,2}$  are the loss tangent of the resonator, substrate1 (region 3 and 7) and substrate2 (region 4 and 8) respectively.

Total dielectric loss( $P_{dt}$ ), in the all region is equal to

$$\Rightarrow P_{dt} = P_{dr} + P_{ds1} + P_{ds2} \quad (2.22)$$

$$\Rightarrow P_{dt} = 2\omega W_{e1}\tan\delta_{dr} + 2\omega(W_{e3} + W_{e7})\tan\delta_{ds1} + 2\omega(W_{e4} + W_{e8})\tan\delta_{ds2} \quad (2.23)$$

$$\Rightarrow \frac{P_d}{2\omega W_e} = \frac{W_{e1}\tan\delta_{dr}}{W_e} + \frac{(W_{e3} + W_{e7})\tan\delta_{ds1}}{W_e} + \frac{(W_{e4} + W_{e8})\tan\delta_{ds2}}{W_e}$$

$$\Rightarrow \frac{1}{Q_{dt}} = \frac{1}{Q_{dr}} + \frac{1}{Q_{ds1}} + \frac{1}{Q_{ds2}}$$

$$\Rightarrow Q_{dt} = \frac{W_e}{W_{e1}\tan\delta_{dr} + (W_{e3} + W_{e7})\tan\delta_{ds1} + (W_{e4} + W_{e8})\tan\delta_{ds2}} \quad (2.26)$$

For special case of two layer dielectric substrate,  $Q_{dt}$  is given by;

1. Suspended substrate case  $\tan\delta_{ds2} = 0$  (substrate2 is assumed to be air region)

and  $Q_{dt}$  is

$$Q_{dt} = \frac{W_e}{W_{e1}\tan\delta_{dr} + (W_{e3} + W_{e7})\tan\delta_{ds1}} \quad (2.27)$$

2. MIC environment case  $Q_{dt}$  can be calculated as follow<sup>4</sup>;

$$hs1=hs2=h/2, \epsilon_{ds1} = \epsilon_{ds2} = \epsilon_{ds}$$

$$\tan\delta_{ds1} = \tan\delta_{ds2} = \tan\delta_{ds}$$

$$Q_{dt} = \frac{W_e}{W_{e1}\tan\delta_{dr} + (W_{e3} + W_{e7})\tan\delta_{ds1}}$$

### 2.3.3 Overall unloaded Q-factor

Once conductor Q-factor and Q-factor due to dielectric losses are calculated, unloaded Q-factor ( $Q_d$ ) can be calculate as follows.

$$\frac{1}{Q_u} = \frac{1}{Q_c} + \frac{1}{Q_{dt}} \quad (2.29)$$

## 2.4 Numerical Results

An analytical formulation is developed, to compute the conductor and dielectric loss, and hence Q-factors ( $Q_c$ ,  $Q_{dt}$  and  $Q_u$ ) in a generalized two layer substrate. Validity of this theory is verified with the data available in literature [13], [1] as the special cases of suspended substrate environment.

The data for  $Q_d$ ,  $Q_c$  and  $Q_u$  of DR in suspended substrate environment are generated taking into account of the losses due to substrate, DR and conductor plates. The dielectric loss due to DR is calculated from graph [14] using method of polynomial interpolation. The polynomial is chosen of third degree as  $Q_d = a_0 + a_1 f_0 + a_2 f_0^2 + a_3 f_0^3$ , where the value of polynomial constant are :  $a_0=39.75625471$ ,  $a_1=-5.112382479$ ,  $a_2=0.251317681$ ,  $a_3=-0.003817681$ . The dielectric loss due to substrate is calculated in same manner from the data given in [15]. Data for  $Q_u$  have also been generated for DR in suspended substrate environment, as a function of tuning plate height(Ha) with different parameter such as bottom airgap (Hs2),  $\epsilon_{dr}$ ,  $\epsilon_{ds}$  etc and they are shown from figure 2.4 to 2.10. These data may be very useful for the design of microwave device containing DR.

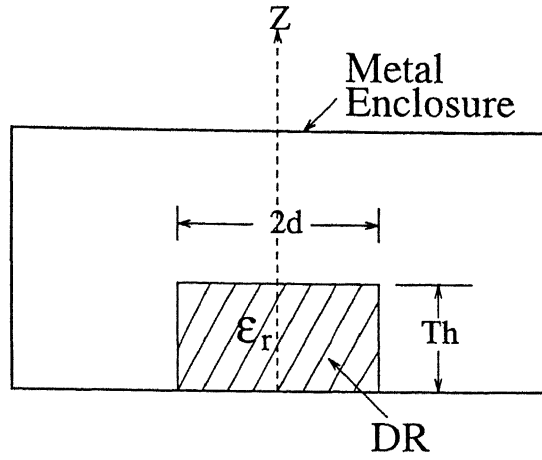


Figure 2.2: DR in Shielded Environment

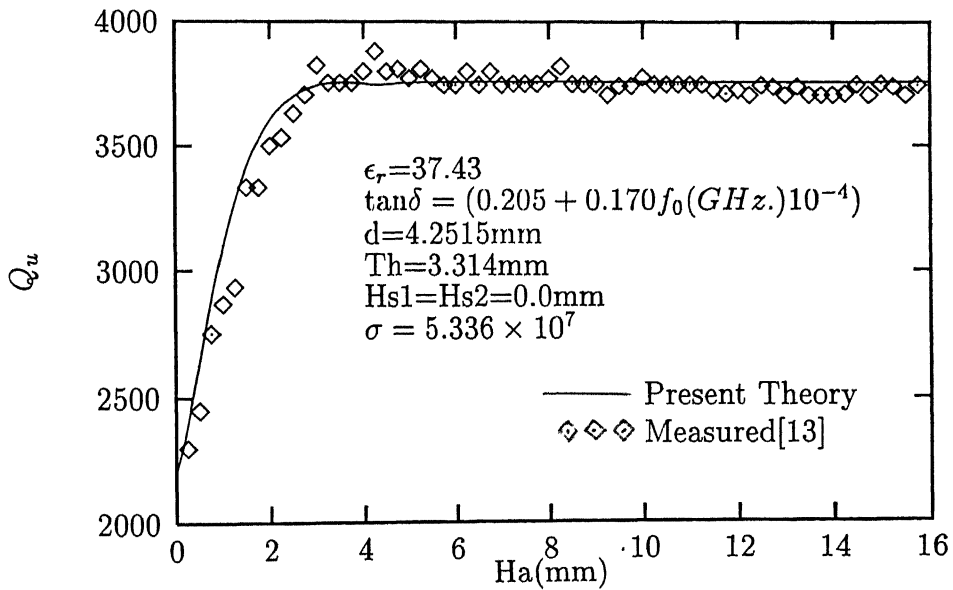


Figure 2.3: Unloaded Q-factor of DR placed in MIC environment

**Table2.1**

$$\sigma=6.14 \times 10^7, Hs1=Hs2=H/2=0.35\text{mm}, \epsilon_{ds1} = \epsilon_{ds2} = 9.6$$

$\epsilon_r$	d (mm)	Th (mm)	Ha (mm)	$\tan\delta_{ds} \times 10^4$	$Q_u$ [1]	$Q_u$ present Theory
34.19	7.49	7.48	0.72	3.02	2470	2449
34.21	6.995	6.95	1.25	3.19	2440	2435
34.02	5.995	5.98	2.215	3.47	2410	2423
36.13	3.015	4 21	10.10	4.22	1980	2168

Table 2.1: Comparison of present theoretical data for  $Q_u$  with that of reported data

### 2.4.1 Validity of present Theory

A comparison between present theory and experimental data for  $Q_u$  available for DR [13] in shielded environment (figure2.2) as special case of DR in suspended substrate environment and is shown in figure 2.3. It shows a good agreement between them for different heights of top plate Ha.

One more comparison is made for DR in MIC environment which is also a special case of suspended substrate environment. Table2.1 shows that comparison. It shows a good agreement with the data reported in [1].

### 2.4.2 Effect of Bottom Airgap (Hs2)

Figure 2.4 shows the variation of  $Q_c$  as function of tuning plate height (Ha) for different Hs2. It is seen from the figure that  $Q_c$  increase with the increase of Hs2. This is because of less field interaction with bottom plate which in interms reduces are the conductor loss.

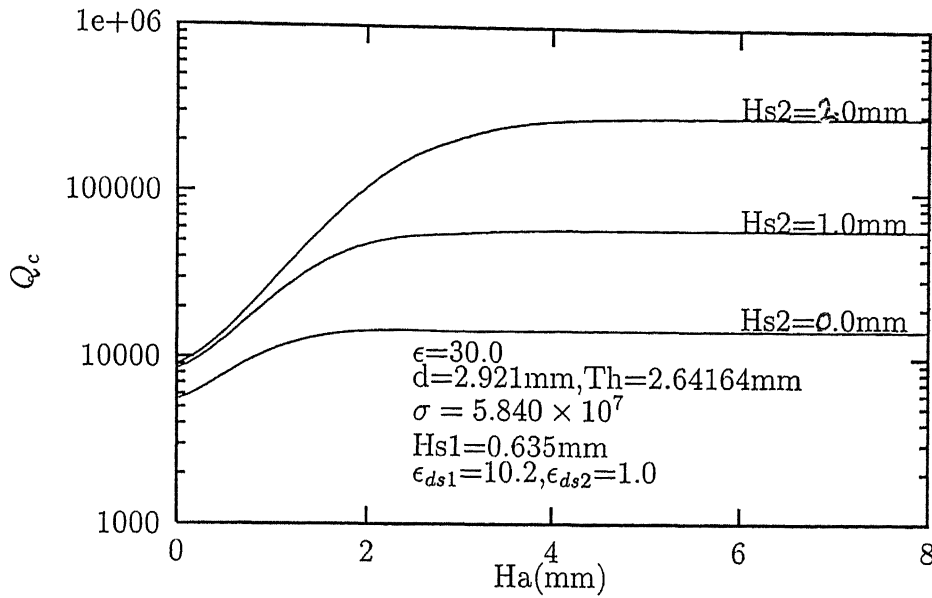


Figure 2.4: Conductor Q-factor of in SS Environment

$Q_d$  decreases due to the fact that the resonant frequency of DR drifts downwards with the increase in  $H_{s2}$ . This causes an increase in electric field distribution in the substrate region which is more lossy than DR, while overall electric energy remain same. Again, the value of conductor Q-factor ( $Q_c$ ) is much higher than  $Q_d$  for fixed value of  $H_a$ . This reflect on calculation of  $Q_u$  where  $1/Q_d$  dominate over  $1/Q_c$ . Hence similar behaviour is observed for  $Q_u$  with increase in  $H_{s2}$ .

### 2.4.3 Effect of Substrates Parameter on $Q_u$

Data for  $Q_u$  is also generated for various value of permittivity of substrate ( $\epsilon_{ds}$ ) and substrate thickness ( $H_{s1}$ ) and is shown in figure 2.6 and 2.7. It is observed from figure 2.6 that the variation of  $Q_u$  increases with the increase of  $H_{s1}$ . That is because more field confines to the substrate, so dielectric loss are more. Effect of permittivity of substrate on the  $Q_u$  is shown in figure 2.7. It is observed from this figure that  $Q_u$  is decreases with the increase in  $\epsilon_{ds1}$ . That is because more and more

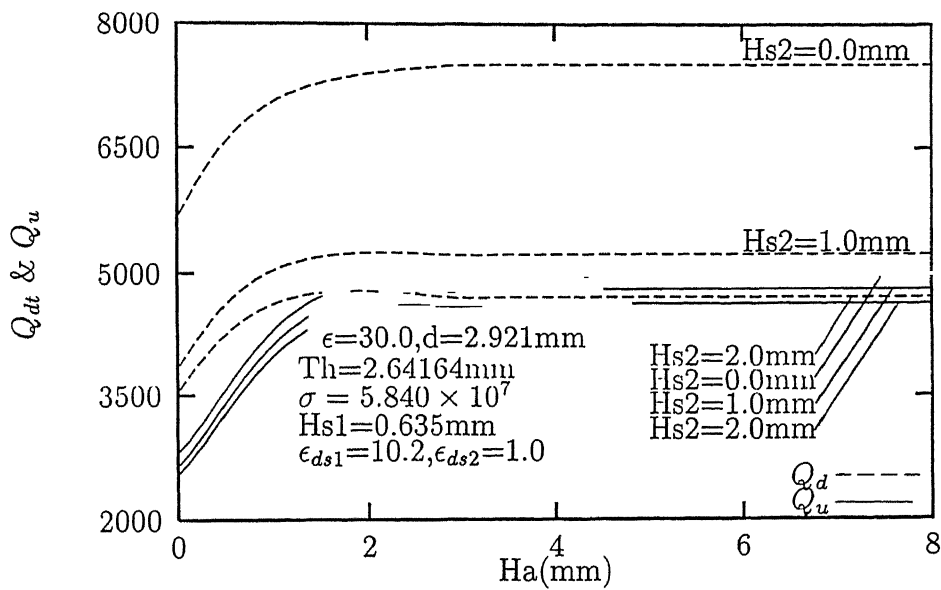
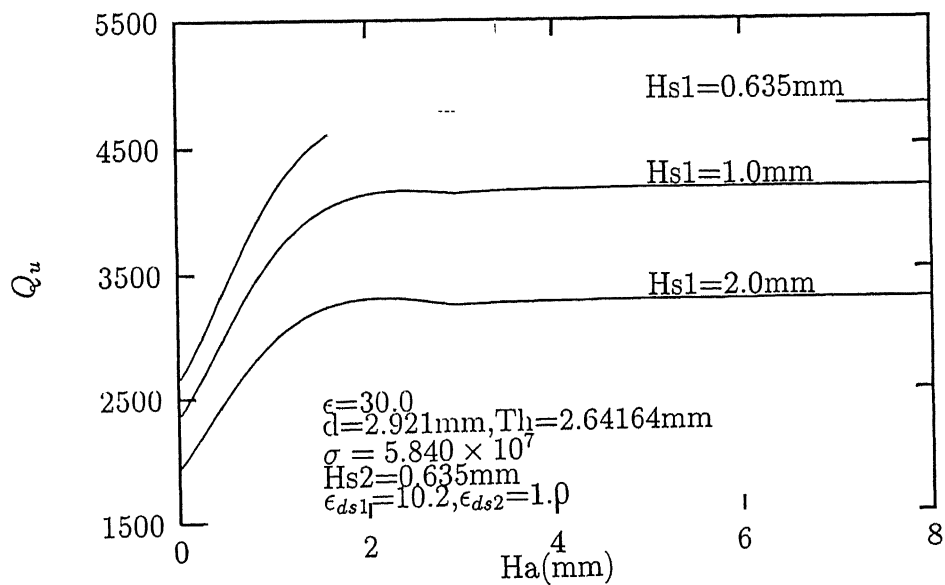


Figure 2.5: Unloaded and dielectric loss Q-factor of in SS Environment



Unloaded Q factor of in SS Environment

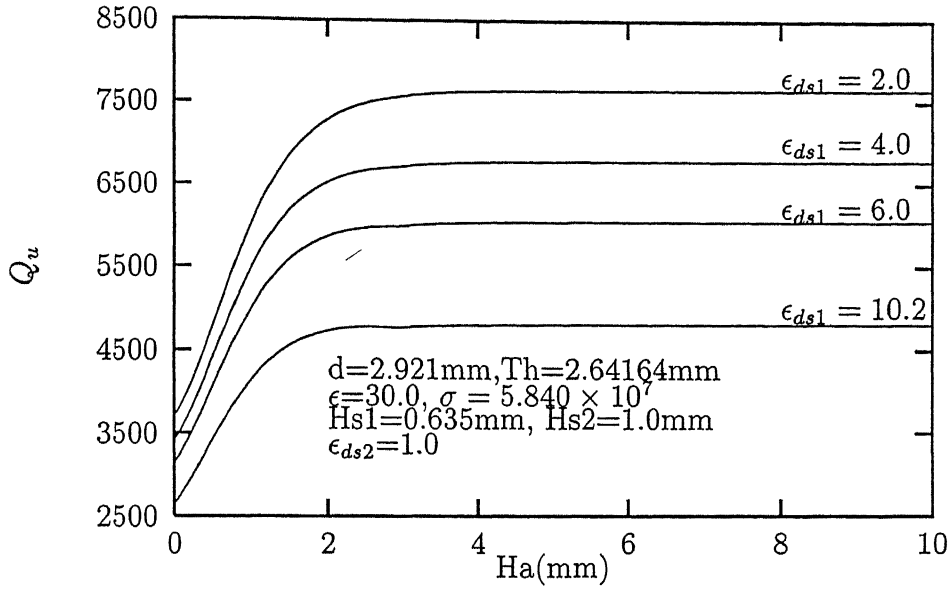


Figure 2.7: Effect of  $\epsilon_{ds1}$  on  $Q_u$

#### 2.4.4 Effect of DR's Parameter on $Q_u$

Effect of various parameter of DR on  $Q_u$  has also been studies. With increase in DR's radius and height,  $Q_u$  increase (figure 2.8 and 2.9). That is because the volume of DR is increased in both case and more energy is confine inside the DR rather than in the substrate or in the air region.

As permittivity of DR increases  $Q_u$  also increase (figure 2.10). As  $\epsilon_r$  increases, more and more energy will be inside the DR. So there will be less conductor and dielectric loss in the shielding wall and substrate respectively.

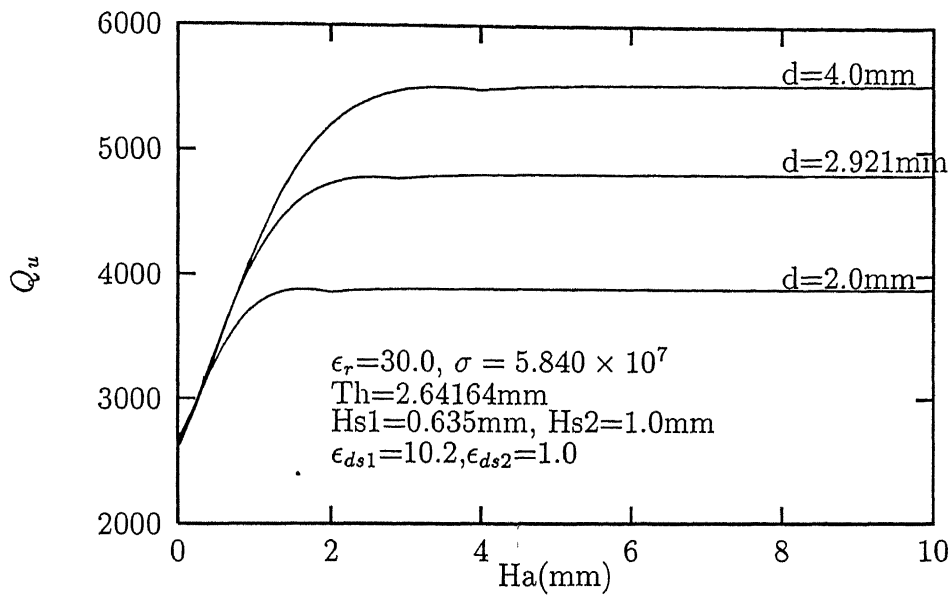


Figure 2.8: Effect of radius of DR on  $Q_u$

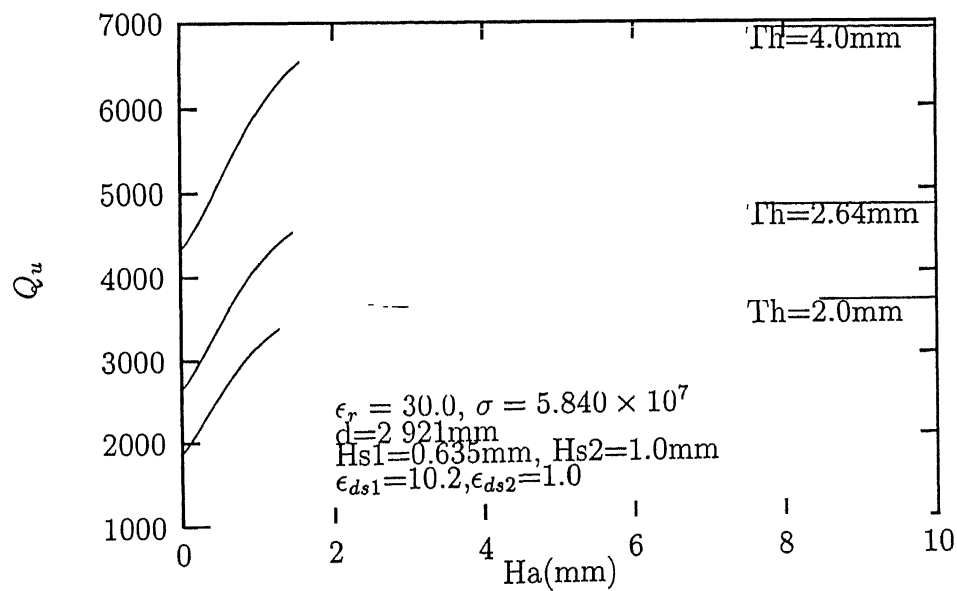


Figure 2.9: Effect of Thickness of DR on  $Q_u$



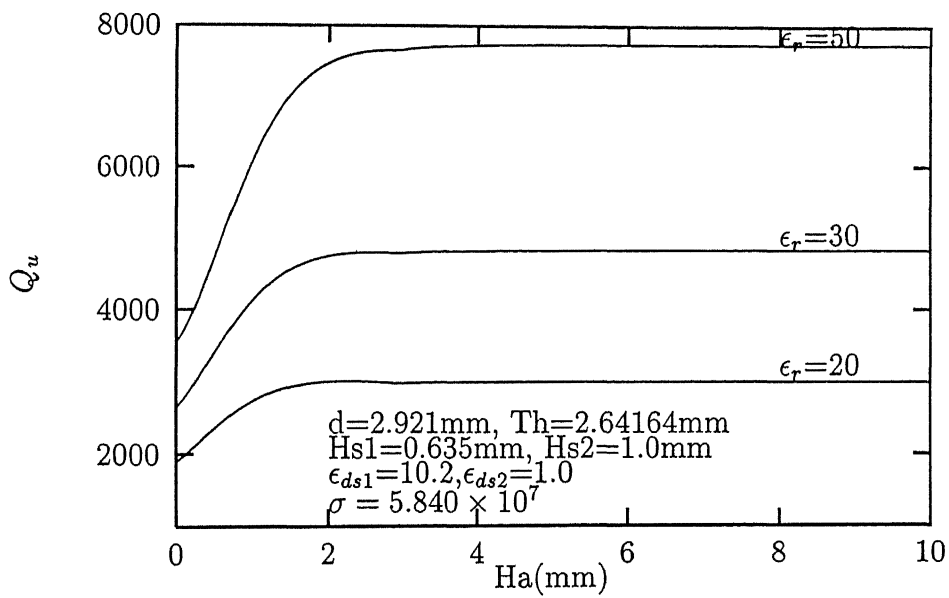


Figure 2.10: Effect of  $\epsilon_r$  of DR on  $Q_u$

# Chapter 3

## Measurement Procedure for Determination of Coupling ( $\beta$ ), $Q_u$ , $Q_{ext}$ and $Q_L$

The precise measurement of coupling coefficient ( $\beta$ ), resonant frequency ( $f_0$ ), and Q-factors is necessary and sufficient for complete characterization of DR in suspended substrate or MIC environment for a particular mode. In this chapter, experimental procedure is discussed to measure these quantities for  $TE_{01\delta}$  mode.

### 3.1 Circuit Parameters: An Introduction

At low radio frequencies the simple resonant circuit can be specified completely by stating the circuit parameters in terms of L, C,  $R_s$  as shown in figure 3.1. The equivalent description of the microwave resonant circuit cannot be so explicit because as in the waveguide or striplines the ordinary concept of voltage and current does not play its usual role. To define the circuit parameters in any microwave problem

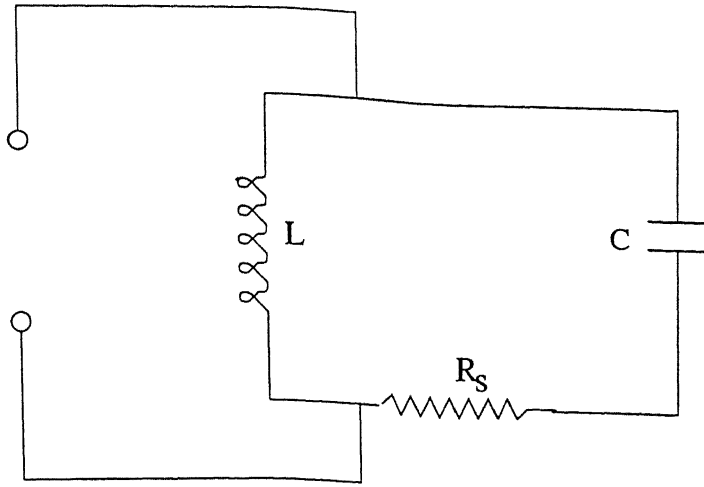


Figure 3.1: Low frequency resonant circuit

in a manner that closely resemble low frequency circuit practice. However, the microwave equivalent circuit concept is complicated by the relatively close spacing of the resonant frequencies of the microwave cavity. In most practical situation the cavity or resonator are used at sufficiently low frequencies so that only one mode is excited at a time, thus making it possible to represent the energy stored in the field of some particular mode by the energy stored in the lumped parameters of the equivalent circuit.

A consideration of low frequency analogue clarifies the meaning of equivalent circuit parameters. The three parameters shown in figure 3.1 can be related to three universally useful relations.

$$\omega_0^2 = \frac{1}{LC} \quad (3.1)$$

$$Q_0 = \frac{\omega_0 L}{R_s} \quad (3.2)$$

$$R_0 = \omega_0 L Q_0 = \frac{(\omega_0 L)^2}{R_s} \quad (3.3)$$

Where  $R_0$  is shunt resistance.

The three quantities defined by these relations can be measured experimentally

resulting in

$$L = \frac{R_0}{\omega_0 Q_0} \quad (3.4)$$

$$C = \frac{Q_0}{\omega_0 R_0} \quad (3.5)$$

$$R_S = \frac{R_0}{Q_0^2} \quad (3.6)$$

The microwave resonant cavity differs that from low frequency circuit in two respects: firstly, the equivalent circuit parameters must be established separately for each mode under consideration and secondly, the quantity  $R_0$  is not uniquely defined due to ambiguity in the meaning of voltage and currents.

## 3.2 Coupling Factor of DR Coupled to Microstrip

In order to effectively use DR in the microwave circuits, it is necessary to have an accurate knowledge of the coupling between DR and transmission line. The  $TE_{01\delta}$  mode of the cylindrical resonator can be easily coupled with microstrip, fin line, magnetic loop and waveguides.

Figure 3.2 shows the magnetic coupling between DR and microstrip line. The resonator is placed on the microstrip. The lateral distance 'y' between DR and microstrip primarily determines the amount of coupling between line and DR.  $TE_{01\delta}$  mode in DR can be approximated by a magnetic dipole of moment M. The coupling between the line and the resonator accomplished by orienting the magnetic moment of the resonator, perpendicular to microstrip plane so that the magnetic lines of the resonator link with those of microstrip line, as shown in figure 3.2. The dielectric resonators placed adjacent to the microstrip line operates like a reaction cavity that reflects the RF energy at the resonant frequency. The equivalent circuit of the resonator coupled to microstrip line is shown in figure 3.3.

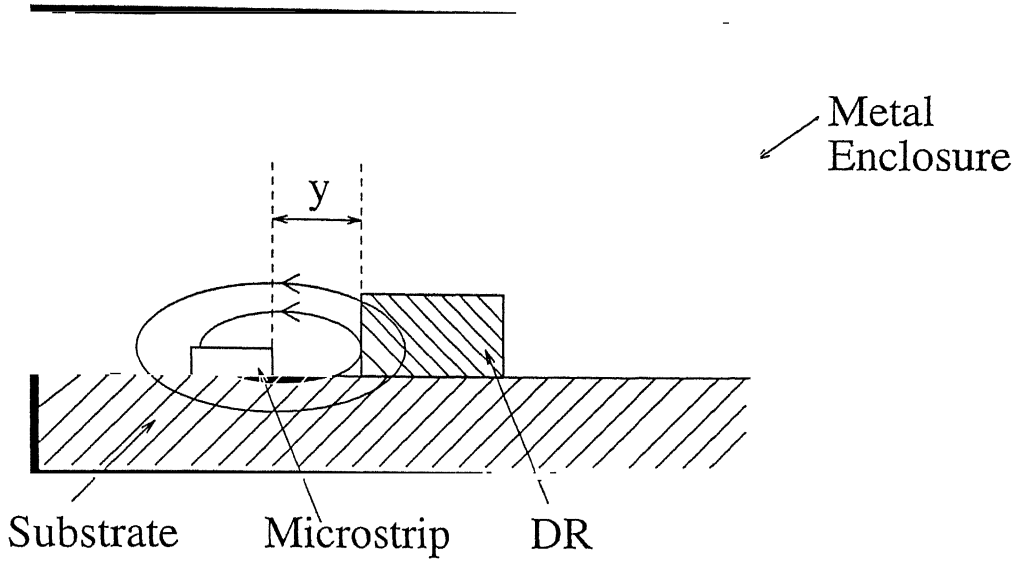


Figure 3.2: Coupling between DR and Microstrip

In figure 3.3  $L_r$ ,  $C_r$  and  $R_r$  are the equivalent parameters of the dielectric resonator,  $L_1$ ,  $C_1$  and  $R_1$  are the equivalent parameters of the microstrip line, and  $L_m$  characterizes the magnetic coupling. The resonator impedance  $Z$  in series with the transmission line is easily determined to be

$$Z_m = j\omega L_1 + \frac{\omega^2 L_m^2}{R_r + j\omega(L_r - 1/\omega^2 C_r)} \quad (3.7)$$

Around resonant frequency  $\omega L_r$  is negligible, so  $Z_m$  is given by

$$Z_m = \omega \cdot Q_u \frac{L_m^2}{L_r} \cdot \frac{1}{1 + jX} \quad (3.8)$$

Where  $X = 2Q_u(\Delta\omega/\omega)$  and unloaded Q-factor, is given by

$$Q_u = \frac{\omega_0 L_r}{R_r} \quad (3.9)$$

$$\omega_0 = \frac{1}{\sqrt{L_r C_r}} \quad (3.10)$$

And S-matrix correspond to figure 1.3 (chapter1) will be

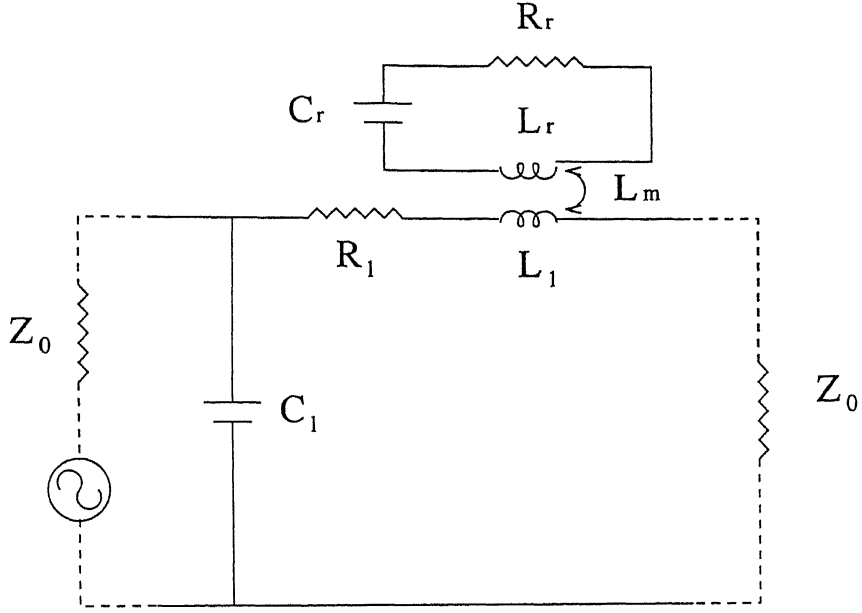


Figure 3.3: Equivalent circuit of DR coupled to microstrip

At the resonance

$\Delta\omega = 0$ , so  $X=0$  and

$$Z_{in} = R = \omega_0 Q_u \frac{L_m^2}{L_r} \quad (3.11)$$

$$S = \begin{bmatrix} \frac{\beta}{\beta+1} & \frac{1}{1+\beta} \\ \frac{1}{1+\beta} & \frac{\beta}{\beta+1} \end{bmatrix}$$

The equivalent circuit of DR coupled with microstrip or suspended strip line can also be represented as resonant circuit shown in figure 1.3.  $L$ ,  $C$ ,  $R$  satisfy the following equations.

$$L = \frac{L_m^2}{L_r} \quad (3.12)$$

$$C = \frac{L_r}{\omega_0^2 L_m^2} \quad (3.13)$$

$$R = \omega_0 Q_u \frac{L_m^2}{L_r} \quad (3.14)$$

From equation 3.12 to 3.15, quantities L, R, and C can be represented in terms of directly measurable parameter  $\beta$ ,  $\omega_0$ , and  $Q_u$  as given below.

$$R = \omega_0 Q_u \frac{2\beta Z_0}{\omega_0 Q_u} = 2\beta Z_0 \quad (3.16)$$

$$L = \frac{R}{\omega_0 Q_u} \quad (3.17)$$

$$C = \frac{Q_u}{\omega_0 R} \quad (3.18)$$

### 3.3 Measurement Setup

Measurement is performed on the Trans-Tech resonator made of D8600 material ( $\epsilon_r=37.43$ ). Same resonator used in the design of oscillator. The resonator is placed on the dielectric substrate and on the plane of symmetry  $pp'$  as shown in figure 3.4. Now this is a two port symmetric and reciprocal device. The substrate is taconic plastic (RT duroid) of thickness of 0.8mm and of relative dielectric constant is 2.18. The characteristic impedance of microstrip line is  $50\Omega$  ( conductor width 2.4mm). The spacing between the resonator and microstrip line (y) is gradually increased in the step of 1mm.

Great care is exercised in measurement of coupling. The first and very important step of the measurement procedure is to measure the scattering parameter (Reflection and Transmission Coefficient) of this two port symmetric device using a Hewlett Packard HP8410 network analyser. About 20-25 point around the resonance are measured for each spacing between DR and microstrip line.

The reflection coefficient( $S_{11} = S_{22}$ ) and transmission coefficient( $S_{21} = S_{12}$ ) measured for three different spacing between DR and microstrip line, are plotted as shown in figure 3.5 and figure 3.6. Both plot shows three peaks/troughs, among these peaks/troughs first will be due to fundamental mode  $TE_{01\delta}$  because of the

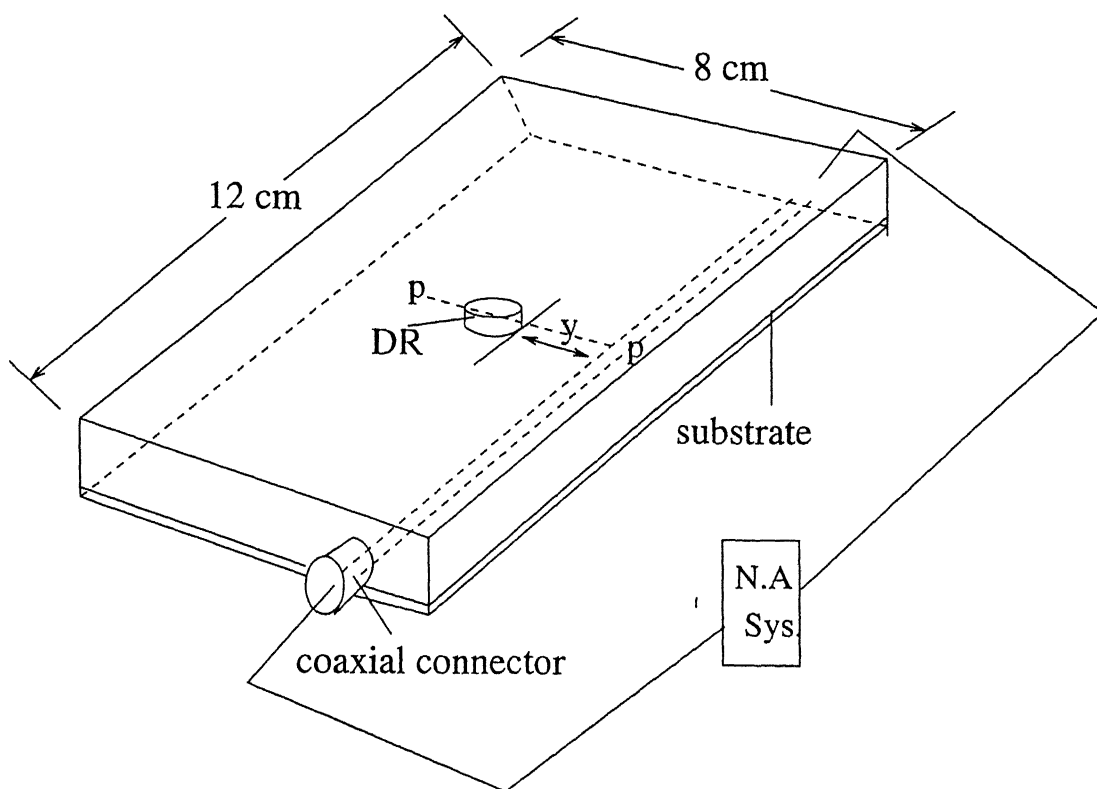
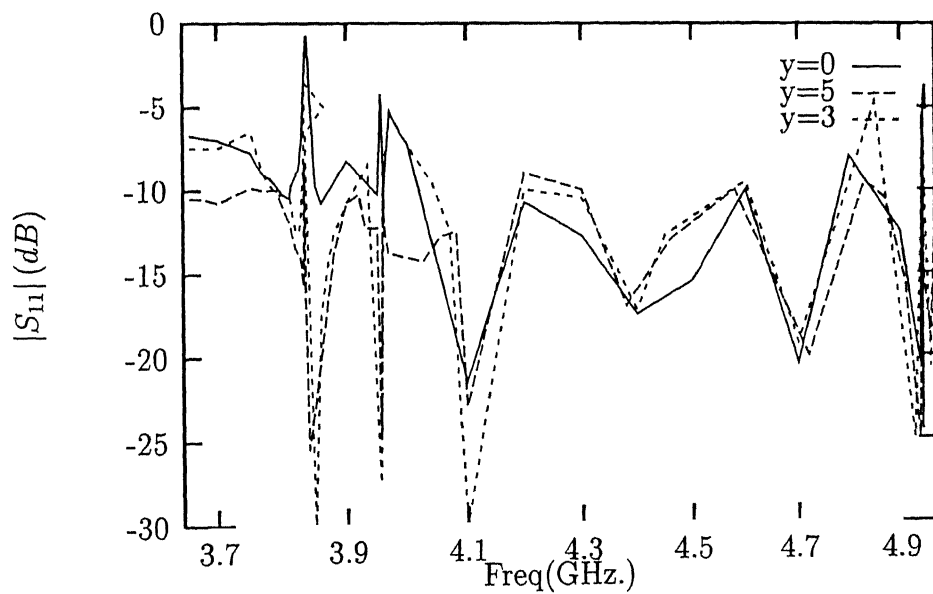


Figure 3.4: Experimental setup





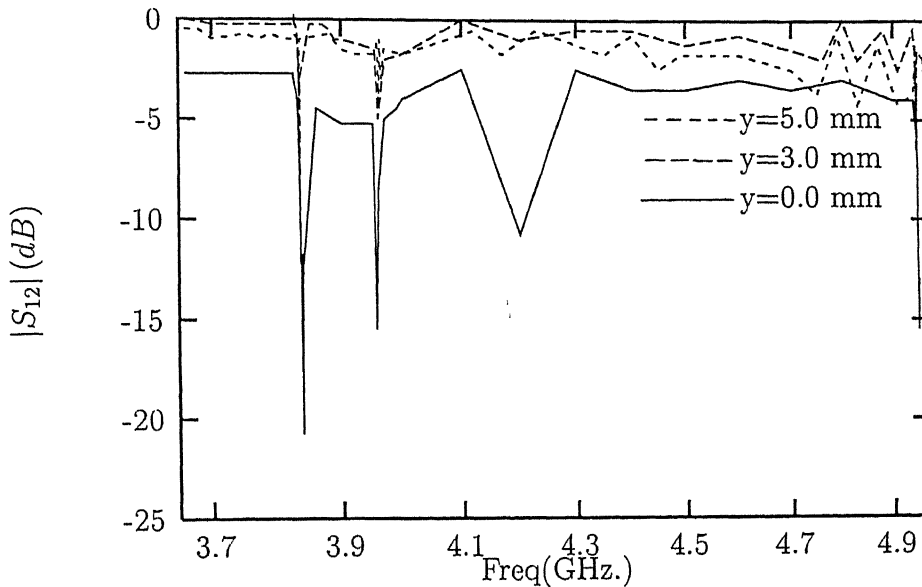


Figure 3.6: Measured  $S_{12}$  for different spacing 'y'

respond to fundamental mode.

- It has been observed that in the absence of top conductor plate second peak vanished. It also observed that second peak is generally not symmetric about resonance. Hence second peak is due to reflection.
- Third peak occurs around 5 GHz with less amplitude compare to first peak so it must be because of higher order mode.

Figure 3.7 and 3.8 shows the measured reflection and transmission coefficient around resonance. It is observed that resonant frequency drift slightly with the spacing  $y$ .

### 3.4 Calculation for $\beta$ , $Q_L$ , $Q_u$ and $Q_{ext}$

The coupling coefficient ( $\beta$ ) can be calculated by either reflection coefficient or transmission coefficient plane as follows:

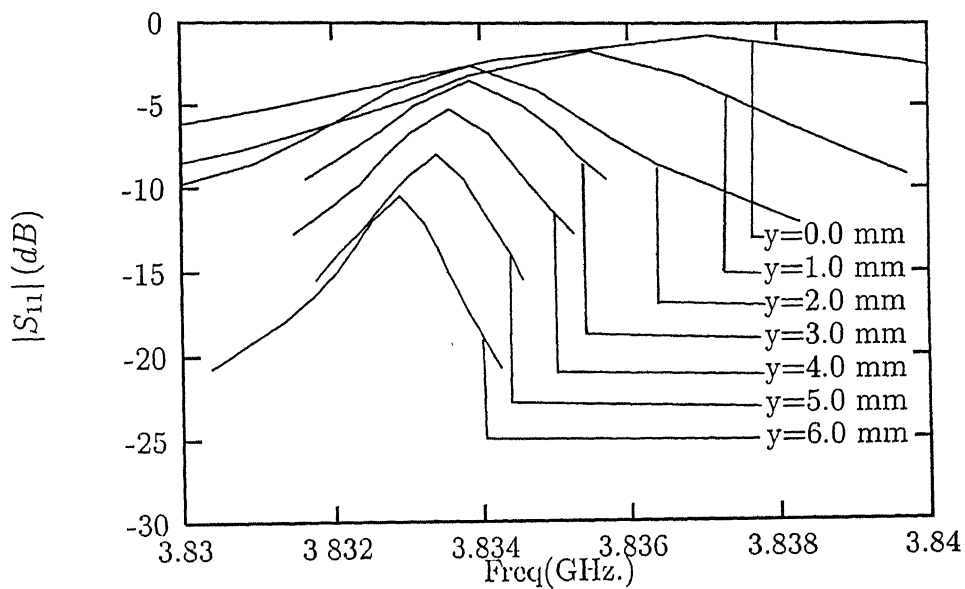
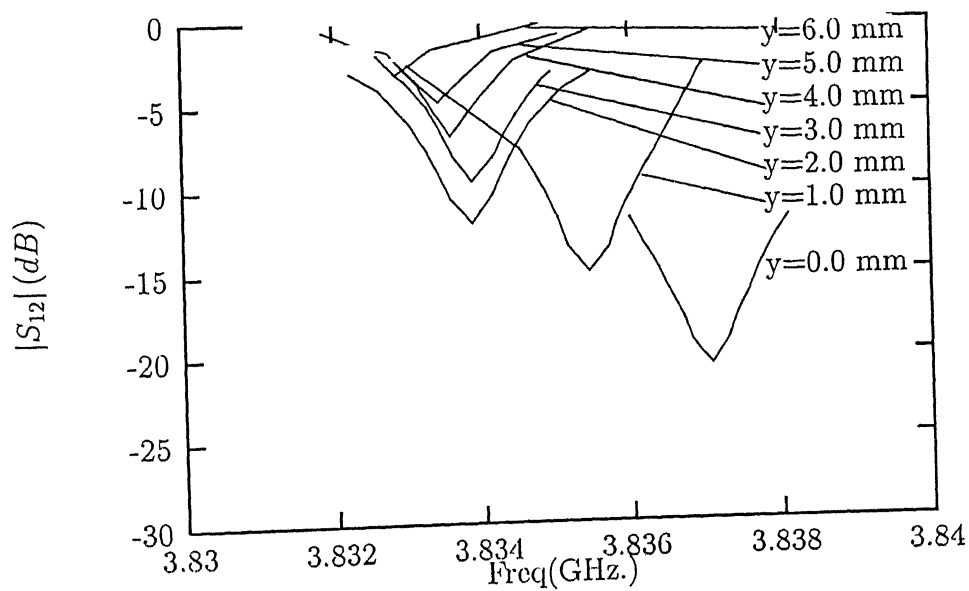


Figure 3.7: Measured  $S_{11}$  around resonance for different spacing 'y'



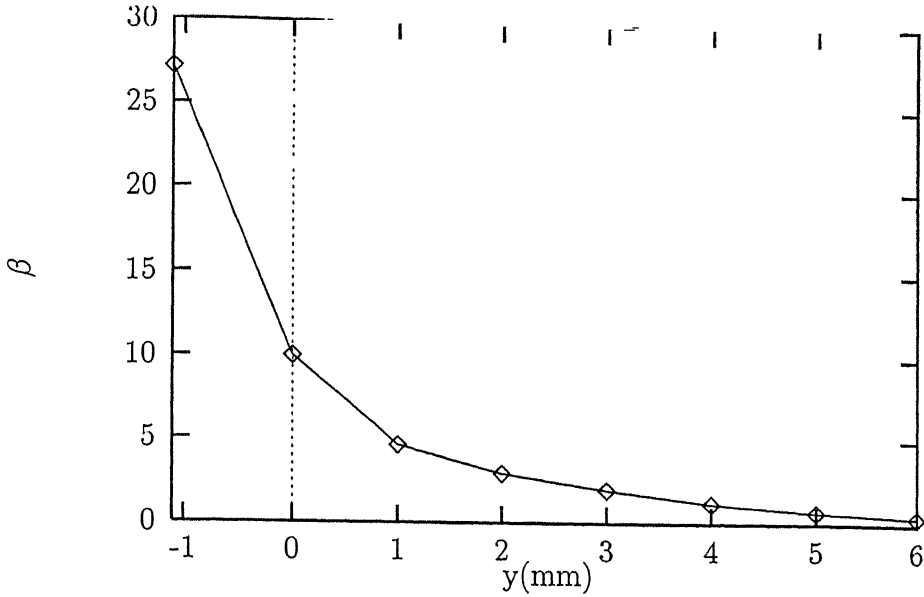


Figure 3.9: Coupling between DR and microstrip

Where  $S_{110}$  and  $S_{210}$  are real quantities representing the reflection and transmission coefficients respectively at the resonant frequency.

Figure 3.9 shows the variation of coupling with the spacing  $y$ . The critical coupling ( $\beta = 1$ ) occurs when the power dissipation in the resonator is equal to the power dissipated in external circuit. The critical coupling corresponds to  $S_{110} = S_{210} = 0.5$ .

As shown in figure 3.10,  $Q_L$  is 3dB point on reflection coefficient plane can be measured directly. from the reflection coefficient plane.  $Q_L$  is 3dB point on reflection coefficient plane.

$$Q_L = \frac{f_0}{f_1 - f_2}$$

$Q_L$  can also be calculated from transmission coefficient plane as follows [16];

$$L_0(\text{dB}) = 20 \log S_{210} \quad (3.20)$$

$$X(\text{dB}) = 20 \log [1 + 10^{-0.1L_0}] \quad (3.21)$$

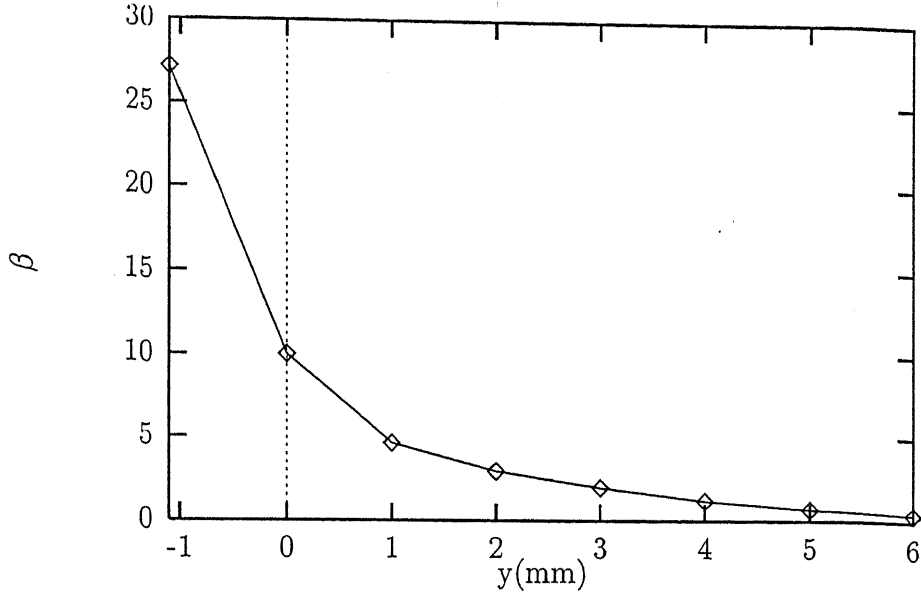


Figure 3.9: Coupling between DR and microstrip

Where  $S_{110}$  and  $S_{210}$  are real quantities representing the reflection and transmission coefficients respectively at the resonant frequency.

Figure 3.9 shows the variation of coupling with the spacing  $y$ . The critical coupling ( $\beta = 1$ ) occurs when the power dissipation in the resonator is equal to the power dissipated in external circuit. The critical coupling corresponds to  $S_{110} = S_{210} = 0.5$ .

As shown in figure 3.10,  $Q_L$  is 3dB point on reflection coefficient plane can be measured directly. from the reflection coefficient plane.  $Q_L$  is 3dB point on reflection coefficient plane.

$$Q_L = \frac{f_0}{f_1 - f_2}$$

$Q_L$  can also be calculated from transmission coefficient plane as follows [16];

$$L_0(\text{dB}) = 20 \log S_{210} \quad (3.20)$$

$$X(\text{dB}) = 3 - 10 \log[1 + 10^{-0.1L_0}] \quad (3.21)$$

Once  $X$  is calculated  $Q_L$  can be calculated from transmission coefficient plane (transmission coefficient Vs. frequency plot), as shown in figure 3.11. Since  $Q_L$  is depen

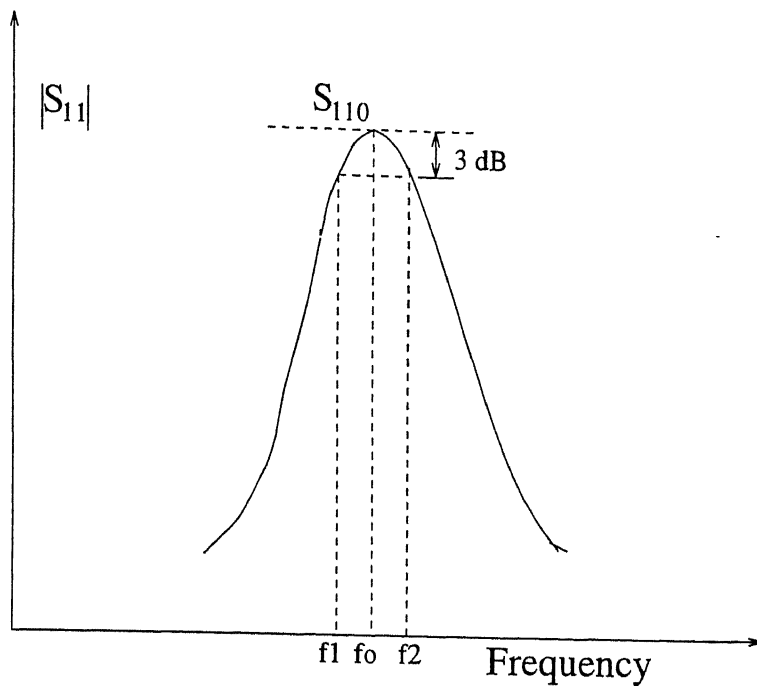


Figure 3.10: Definition of various terms in reflection plane

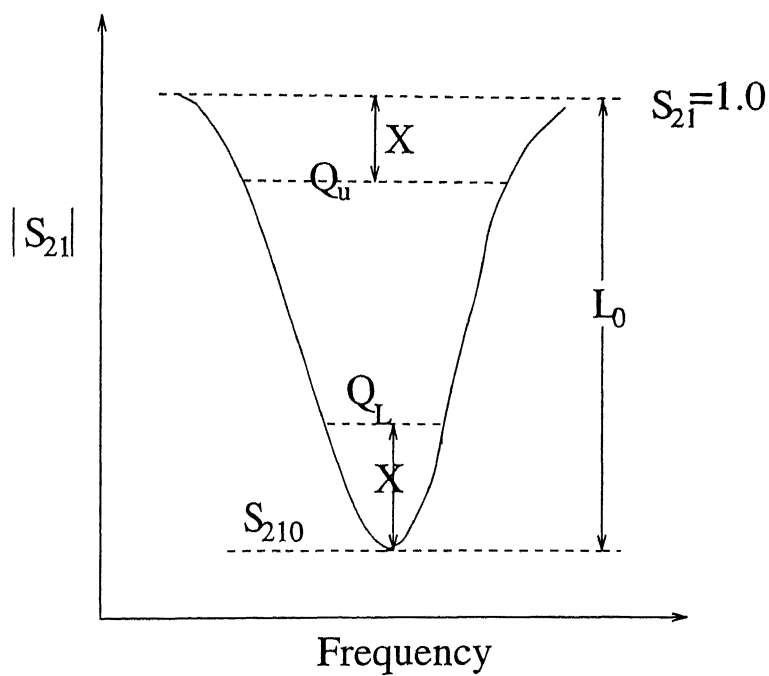


Figure 3.11: Definition of various terms in transmission plane

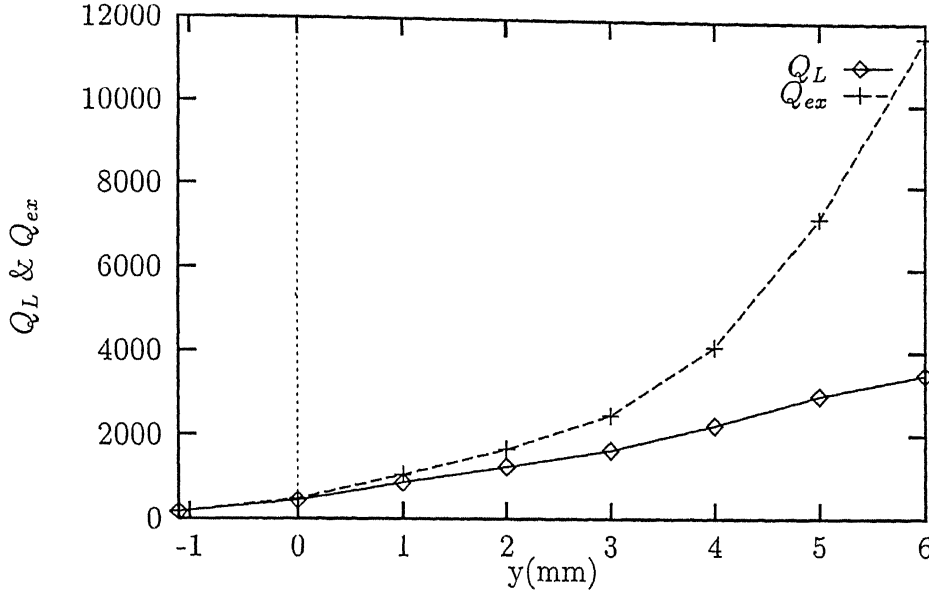


Figure 3.12: Variation of  $Q_L$  and  $Q_{ext}$  of Loaded DR

dent on spacing  $y$ , so generally  $X$  is an odd figure; e.g 2.87, 2.674 etc, and, hence, it is difficult to find this point ( $X$ ) accurately on transmission coefficient plane. So it is better to calculate  $Q_L$  in reflection coefficient plane.

Once  $\beta$ ,  $f_0$ , and  $Q_L$  are calculated the other Q-factors,  $Q_u$  and  $Q_{ext}$  can be calculated as follow;

$$Q_{ext}\beta = Q_u = Q_L(1 + \beta)$$

The variation of  $Q_{ext}$  and  $Q_L$  are plotted with spacing  $y$  and is shown in figure 3.12. Table 3.1 shows  $Q_u$  and coupling ( $\beta$ ) for different spacing between resonator and microstrip. The difference between the largest and smallest value of  $Q_u$  is less than 3%. That is, the  $Q_u$  of the covered DR is supposed to be depend only on the distance from resonator to the top and bottom conductors, and not on the lateral position of DR. So it should be almost constant.

y(mm)	$\beta$	$Q_u$	y(mm)	$\beta$	$Q_u$
-1.1	27.12	4848	3.0	1.99	4919
0.0	9.99	4880	4.0	1.19	4906
1.0	4.62	4880	5.0	0.69	4977
2.0	2.95	4818	6.0	0.43	4908

Table 3.1: Data for coupling and unloaded Q-factor of DR coupled with microstrip

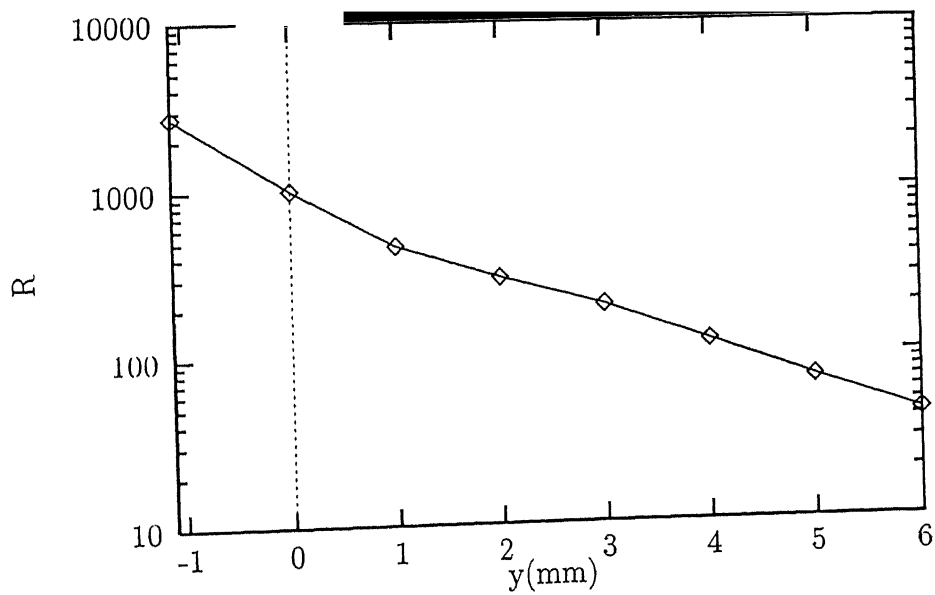


Figure 3.13: Equivalent resistance of DR coupled to microstrip

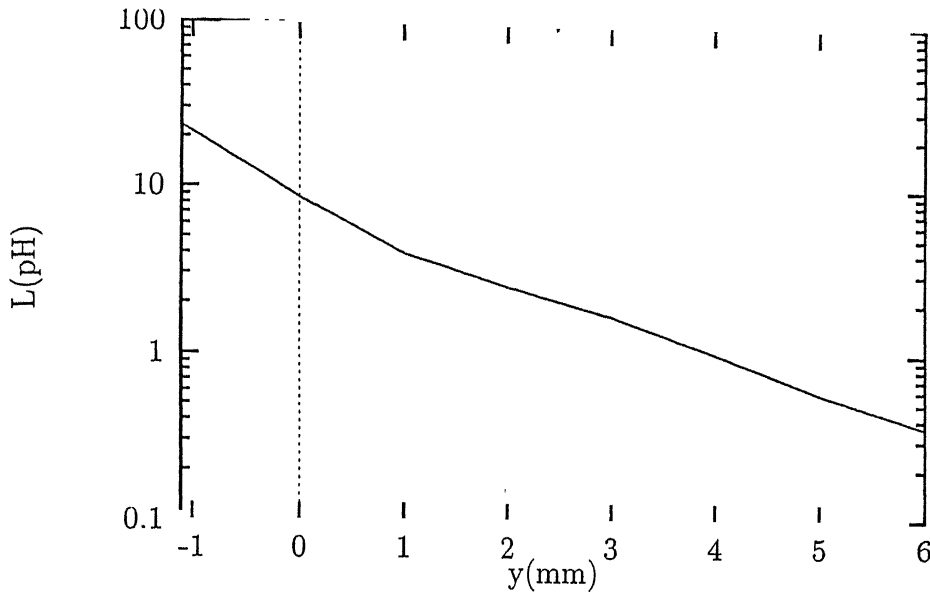


Figure 3.14: Equivalent inductance of DR coupled to microstrip

### 3.5 Results

The equivalent circuit parameter ( $R$ ,  $L$ , and  $C$ ) of the DR coupled to microstrip, on plane  $pp'$  as shown in figure 1.2, are calculated directly from measurable quantity  $\beta$ ,  $f_0$  and  $Q_u$ . These parameters are plotted against lateral spacing of DR from microstrip as shown in figure 3.13 to figure 3.15. All these plot might be very useful in the design of microwave system containing the DR, since these give the direct value of the circuit parameters. It is observed from the figure 3.13 that  $R$  is decreasing with the increase of spacing  $y$ . As spacing  $y$  increases lesser power will be coupled to DR so that dielectric loss is lesser. Hence  $R$  is going downwards with the increase in spacing  $y$ . Again, it is seen from figure 3.11 that the equivalent inductance  $L(=L_m^2/L_r)$  also decrease with increase in  $y$ . This is because of lesser mutual coupling ( $L_m$ ) taking place when  $y$  increases. The equivalent capacitance increase with the increase in spacing  $y$  is shown in figure 3.15. Here, increase in equivalent capacitance is due to fact that mutual coupling between DR and microstrip ( $L_m$ ) decreases with the increase in spacing (equation 3.13).



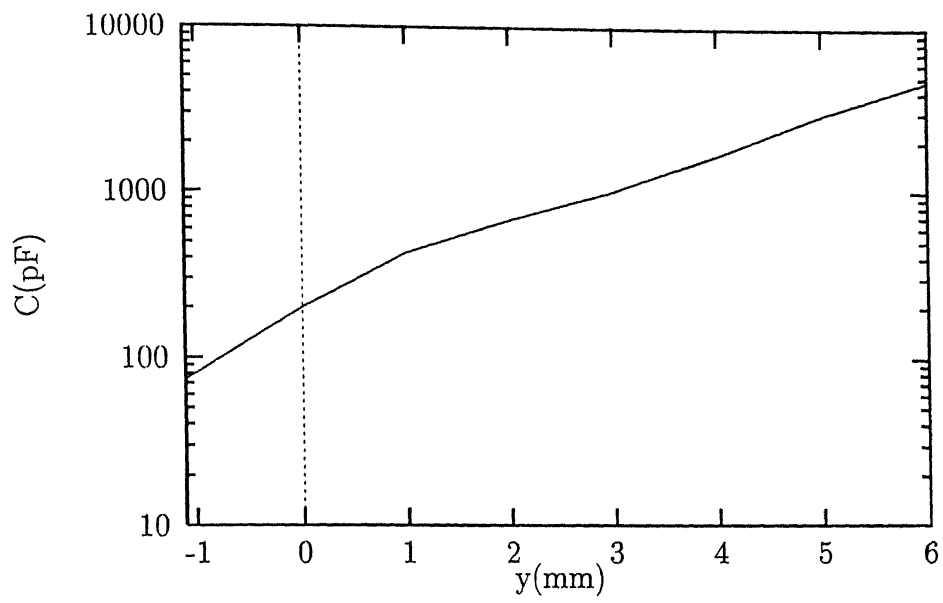


Figure 3.15: Equivalent capacitance of DR coupled to microstrip

# Chapter 4

## Design and Fabrication of DR Oscillator

The transistorized oscillators can be classified according to whether their design is based on linear device(BJT or FET) parameters such as the S- and Y-parameters, or based on large signal behavior of the transistor. The former category is sometimes known as the linear oscillator where as the later is sometimes referred to as the power or large signal oscillator.

### 4.1 Theory of Oscillation

A simple and popular method of oscillator to place a tuning resonator across the input terminals of two port network is shown in figure 4.1. The condition for oscillation for such oscillator can be expressed as [17]

$$K < 1 \quad (4.1)$$

$$\Gamma_1 S'_{11} = 1 \quad (4.2)$$

If and only if

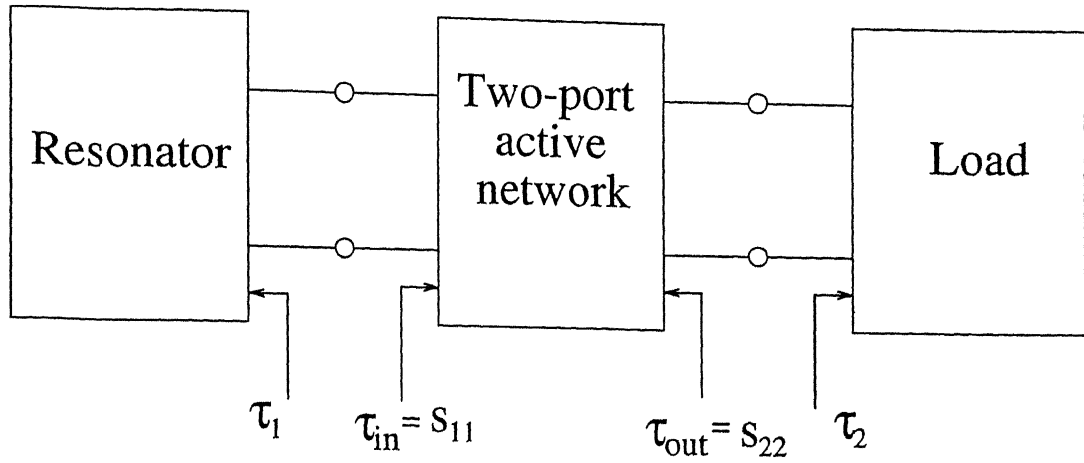


Figure 4.1: Block diagram of an oscillator [17]

In order to start and sustain the oscillations it is necessary that

$$|\Gamma_1| > \left| \frac{1}{S'_{11}} \right| \quad (4.4)$$

$S'_{11}$  and  $S'_{22}$  are given by

$$S'_{11} = S_{11} + \frac{S_{12}S_{21}\Gamma_2}{1 - S_{22}\Gamma_2} \quad (4.5)$$

$$S'_{22} = S_{22} + \frac{S_{12}S_{21}\Gamma_1}{1 - S_{11}\Gamma_1} \quad (4.6)$$

The stability factor K, known as Rollet stability factor is defined as

$$K = \frac{1 - |S_{11}|^2 - |S_{22}|^2 + |\Delta|^2}{2|S_{21}S_{12}|} \quad (4.7)$$

Where  $\Delta = S_{11}S_{22} - S_{21}S_{12}$ , and  $S_{ij}$  are S-parameters of the device.

The equation 4.2 to 4.4 are equivalent to Barkhausen criterion for oscillator design.

Equation 4.2 can also be written as  $R_{in} + R_1 = 0$  and  $jX_{in} + jX_1 = 0$  Or

$$R_{in} = -R_1 \quad \text{and} \quad X_{in} = -X_1 \quad (4.8)$$

Where  $R_{in}$ ,  $R_1$ , and  $X_{in}$ ,  $X_1$  are shown in figure 4.2.

The stability factor K of the active network should be less than unity in order to

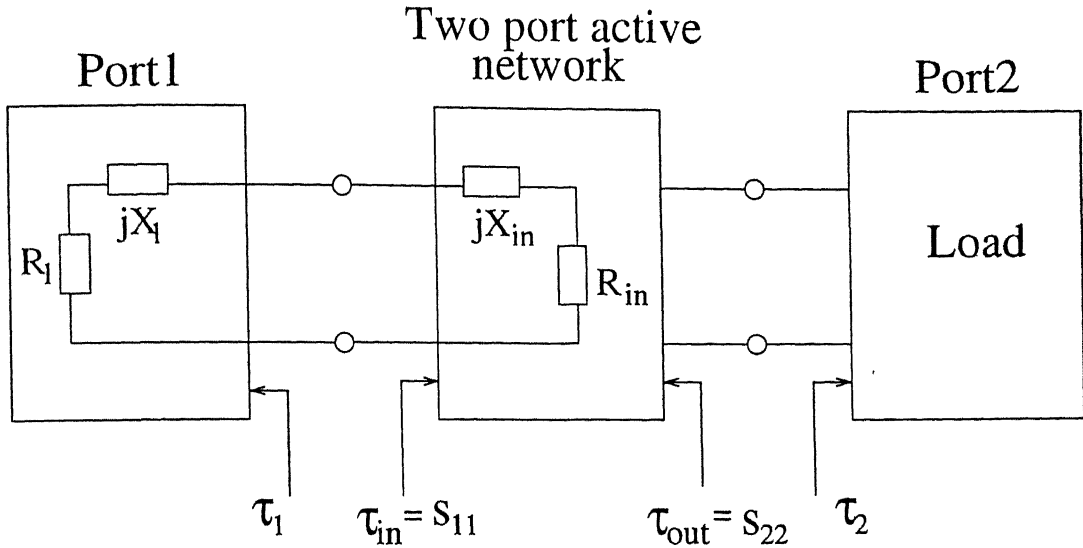


Figure 4.2: Oscillation in port 1 [17]

a bypass capacitor) should be added. The positive termination  $\Gamma_1$  and  $\Gamma_2$  must be designed in such a way that the input and output ports are resonating simultaneously at the same frequency.

## 4.2 Oscillator Design

In the design of stable oscillator, DRs <sup>generally used</sup> are as frequency determining circuit, feedback circuit, or a matching circuit element. This reduces the size as well as cost provided we should be able to eliminate undesirable features of mode jumping and hysteresis. A stable TDRO has a high efficiency circuit of more simple construction, making it an obvious choice.

An oscillator circuit can be represented as either a series or parallel resonant circuit. The commonly used table TDRO's can be divided in two part: one using the DR as series element, and other using the DR as parallel feedback element. In this thesis, the oscillator is designed using former type. Figure 4.3 shows the basic circuit diagram of a series feedback transistor DRO.

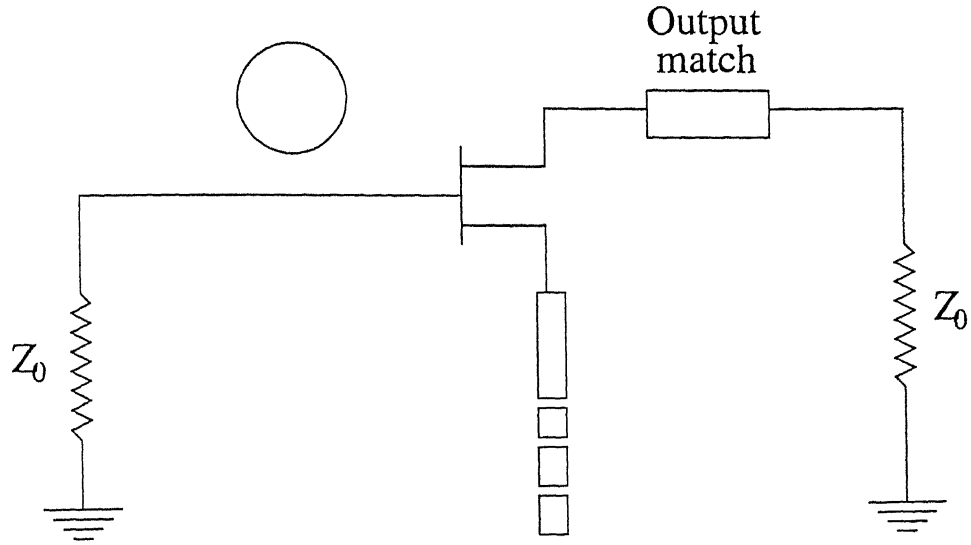


Figure 4.3: DR as a series feedback element in DRO [16]

## 4.3 Choice of transistor and its biasing

### 4.3.1 Choice of transistor

In the design of any active circuit, choice of transistor (or any other active element) is very critical. Because it decide the maximum available gain and noise figure of the device.

So we first select a transistor of desired capability and frequency range. A FET NE70083 [NEC] is selected for oscillator design with following specification at 4GHz.

Noise Figure (NF)=0.7 dB

Max. available Gain(G)=14.0dB

Output power (Po)=14.5dBm

Power dissipated (Pd)=400 mW

And S-parameter at  $V_{ds} = 3V$  and  $I_{ds} = 30mA$  are

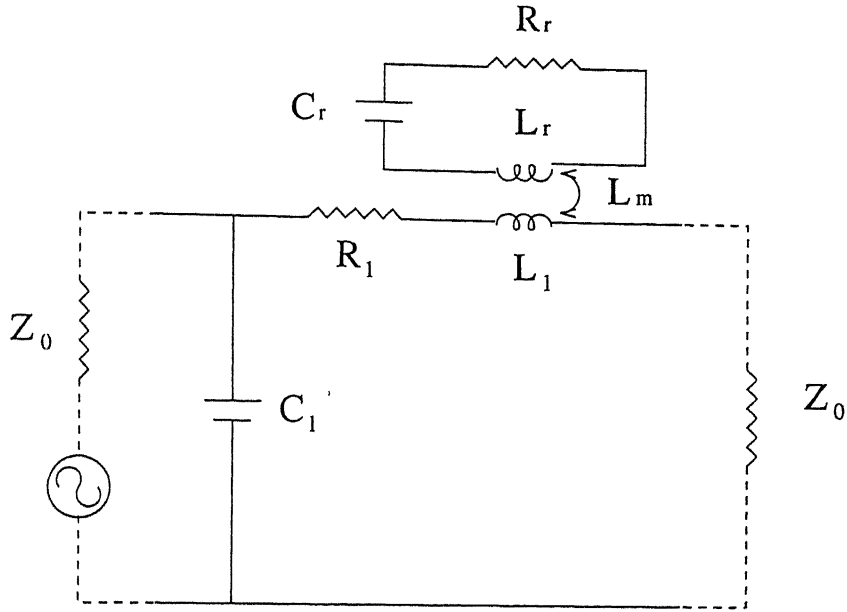


Figure 4.4: Device characteristic

### 4.3.2 Biasing of the transistor

For the design of biasing circuit we fixed the Q-point, from device characteristic, which decide available gain and actual S-parameter. Figure 4.4 shows the Q-point selected as  $V_{ds} = 3V$  and  $I_{ds} = 30mA$ . At this point S-parameters are given above. Figure 4.5 shows the circuit diagram of oscillator. The value R, L,  $C_1$  and  $C_2$  are calculated as follow.

$C_1$  and  $C_2$  must act as short-circuit at 4.0 GHz. and as a open circuit at dc.

$$\frac{1}{\omega C} \cong 10(\text{say}) \text{ at } 4 \text{ GHz.}$$

$$\frac{1}{\omega C} \approx \infty \text{ at dc}$$

$$C_1 \text{ and } C_2 \approx 0.1 \text{ nF} = 100\text{pf}$$

Inductor (L) should be act as a short circuit for dc and o/c at 4 GHz., so that no output signal should leak to ground.

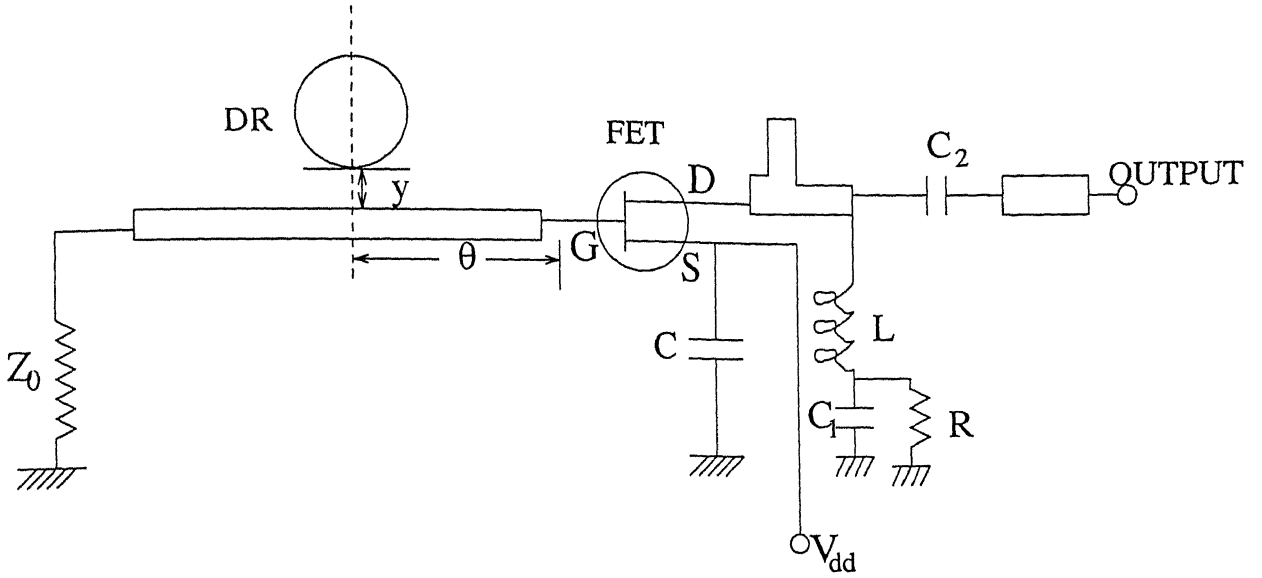


Figure 4.5: circuit diagram of oscillator [18]

R can be calculated as follow

$$i=30 \text{ mA} , V_{dd} = 6V \text{ and } V_{ds} = 3V$$

$$\text{so } V_s=3.0V \text{ and } R= V_s/i \text{ or } R=100\Omega$$

## 4.4 Stability Consideration

The stability factor  $K$  decides whether the device will work as oscillator or not. From the S-parameter  $K$  is calculated as 0.3618. The value  $K$  is less than unity and device is potentially stable. However  $K$  is not much smaller than unity, and this mean that the choice of input and output impedance that will make the device oscillate is limited. In order to make the transistor more liable to oscillate at resonant frequency a capacitive feedback from source is added to ground, this capacitor also work as bypass capacitor.

This capacitor is normally chosen to have a reactance of the same order of magnitude as the input impedance of FET. For transistor NE70083, their are two source

of C is chosen the required microstrip stub can be easily calculated.

#### 4.4.1 Calculation of S-parameter with feedback capacitor

First we convert device S-parameter to Z-parameter as follow

$$Z_m = Z_0(I + S_m)(I - S_m)^{-1} \quad (4.9)$$

Where  $Z_0$  is the characteristic impedance of microstrip line and equal  $50\Omega$ . Converted Z-parameters are given below.

$$Z_m = \begin{bmatrix} 58.02\angle-73 & 4.25\angle-40 \\ 320.6\angle27 & 9.78\angle-49 \end{bmatrix}$$

Since the input impedance of the device is of the order of  $Z_{11}=58.5\angle-73^\circ$ , The impedance of the feedback circuit  $Z_c$  (impedance of capacitance) =  $-j30\Omega$  Then the feedback network can be represented by Z-matrix,  $Z_f$ , given by

$$Z_f = \begin{bmatrix} -j30 & -j30 \\ -j30 & -j30 \end{bmatrix}$$

The overall Z-matrix of transistor with this feedback capacitor is given by displayed equation:

$$Z = Z_m + Z_f$$

Or

$$Z = \begin{bmatrix} 87.34\angle-78.8 & 32.89\angle-84.3 \\ 308.1\angle22 & 115.1\angle-58.8 \end{bmatrix}$$

Now the S-matrix corresponding to this Z-matrix can be obtained as follow.

$$S = (Z + Z_0I)^{-1}(Z - Z_0I) \quad (4.10)$$

The S-parameter of the transistor with feedback are



#### 4.4.2 Design of open circuit stub to obtain capacitance at source terminals

$X_c$  was chosen in the previous section as  $-j30\Omega$

$$Z_{oc} = -jZ_0 \tan \beta l$$

$$\text{Let } Z_0 = 60\Omega$$

Here two parallel stub are designed at the source terminal of transistor. So  $X_c$  for each stub is

$$X_c = -j60\Omega$$

$$-j60 = -j60 \cot \beta l, \text{ or } \beta l = \pi/4$$

Assume microstrip line is a quasi TEM line, so

$$\beta = 2\pi/\lambda, \text{ or } l = \lambda/8$$

$$\lambda_{(z_0=60)} = 5.7847 \text{ cm, so}$$

$$\text{length of each stub } (l_s) = 7.23 \text{ mm}$$

$$\text{Width of stub } (W) = 1.9 \text{ mm}$$

### 4.5 Input and Output Matching Network

The equivalent circuit of input/output matching network is shown in figure 4.6. Using Y-parameter converted from S-parameter, the device impedance  $Z_D$  seen from terminal G can be calculated as [17].

$$Z_D = \frac{1 + Y_{22}Z_{out}}{Y_{11} + (Y_{11}Y_{22} - Y_{12}Y_{21})Z_{out}} \quad (4.11)$$

And the oscillation condition is given by

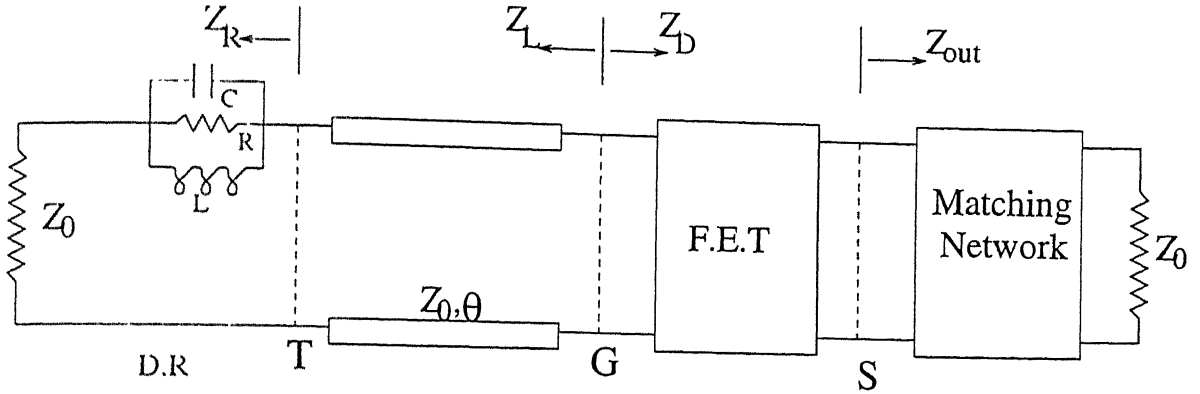


Figure 4.6: Equivalent Circuit of Oscillator [17]

From the two equations given above, the combination of output impedance,  $Z_{out}$ , and the device impedance,  $Z_D$ , is optimized for the maximum negative resistance of  $Z_D$ . The optimum combination of  $Z_{out}$  and  $Z_D$  is obtained as follows:

$$Z_{out}=5+j60(\Omega)$$

$$Z_D=-97.8-j15.13(\Omega)$$

Once  $Z_{out}$  and  $Z_D$  are found output and input matching network can be designed.

#### 4.5.1 Design of Output Matching Network

The output matching network is designed with a wider microstrip or lesser characteristic impedance ( $Z_0 = 40\Omega$ ) line. Stub is designed with a high impedance line ( $Z_0 = 60\Omega$ ). To minimize the transition interaction between the shunt stub and series transmission line, the shunt stub are usually balanced along the series transmission line. Two parallel shunt stubs of same admittance instead of the single stub must be provided for that purpose. The dimensions of stub and line are given below.

Length of the line ( $l_2$ )=1.058 cm Length of the each stub ( $l_3$ )=1.944 cm

#### 4.5.2 Design of Input Matching Network

W(mm)	H(mm)	$\epsilon_{eff}$	$Z_0 (\Omega)$	$\lambda_g = \lambda_0 / \sqrt{\epsilon_{eff}}$
1.9	0.8	1.83	60.0	5.7847
2.4	0.8	1.854	50.0	5.7468
4.0	0.8	1.91	40.0	5.6621

Table 4.1: Data for width and effective dielectric constant of microstrip

$Z_R$  found from the smith chart is given by  $102.5\Omega$ .

The distance of DR from the Gate( $\Theta$ )= $\beta l_1=0.097\pi$  radian so  $l_1 = 0.485\lambda$

One end of the line is terminated with the matched load ( $50\Omega$ ), so that at any distance, this line offers pure resistance ( $50\Omega$ ). Distance of DR from the termination of line ( $l_4$ ) is chosen to be equal to distance of DR from the gate  $l_1$ . This makes the DR symmetric with the line as characterized in chapter 3 (figure 1.3) and effect of the side wall is also minimized. Now the distance between line and DR 'y' is selected in such a way that it simulates an impedance of  $52.5\Omega$ . From the from figure 3.13 this distance is found to be  $y=5.6\text{mm}$ . The PCB layout of the circuit is shown in figure 4.7.

Width of microstrip line (W), effective dielectric constant ( $\epsilon_{eff}$ ) and guided wavelength ( $\lambda_g$ ) for various characteristic impedance ( $Z_0$ ) are given in table4.4.  $Z_0$  and  $\epsilon_{eff}$  has been calculated using synthesis formula given in [17] and [19] respectively.

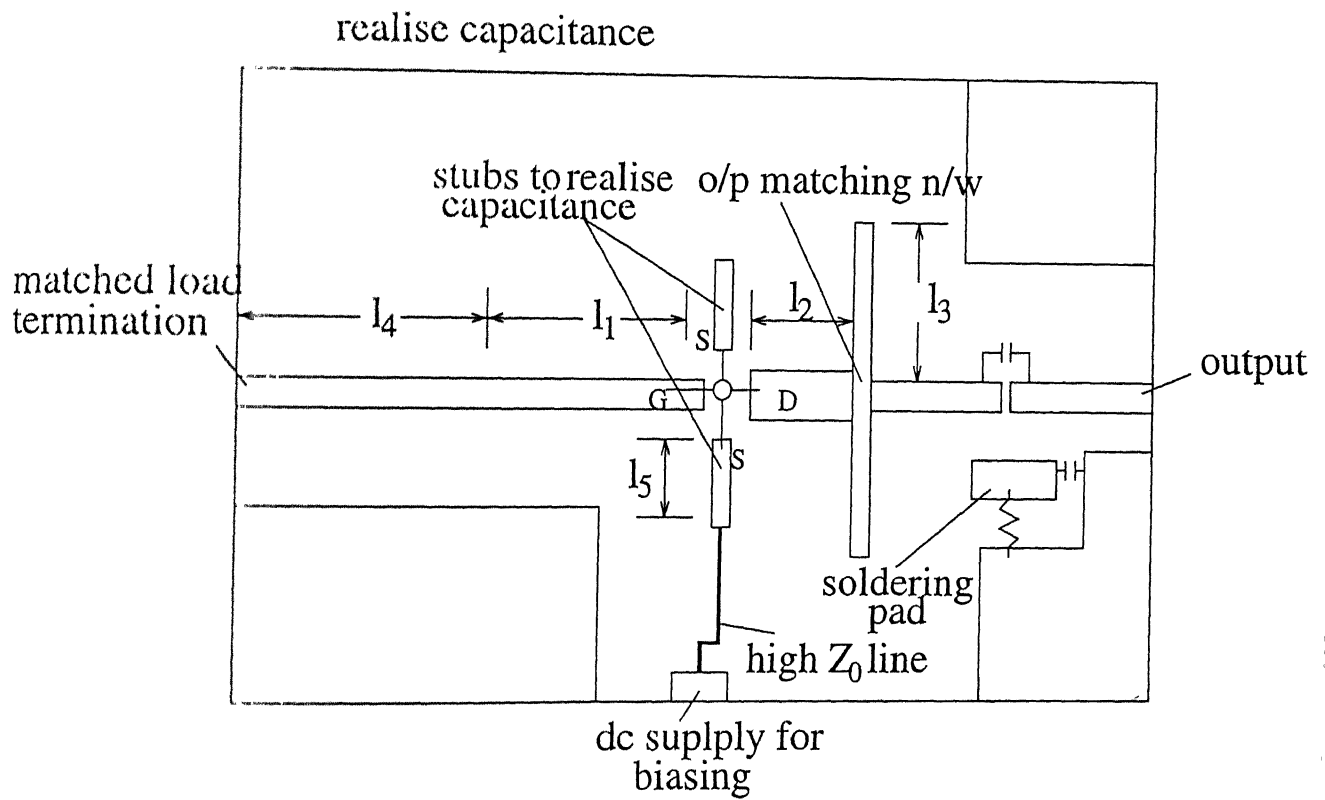


Figure 4.7: PCB layout of the oscillator circuit

# Chapter 5

## Conclusion and suggestion for future Development

### 5.1 Conclusion

In the design of microwave circuits, Q-factor is always a important parameter. Dielectric loss in the dielectric resonator (DR) and substrate and conductor loss in the top and bottom ground plate for the DR placed in the suspended substrate environment have been calculated in the present work. Thereafter, various Q-factor ( $Q_u$ ,  $Q_c$  and  $Q_d$ ) have been calculated. Subsequently, frequency dependent dielectric losses in DR and substrate have been incorporated. Effect of various parameters of DR and substrate on quality factor has also been studied.

An experimental procedure to measure the coupling between DR and microstrip for  $TE_{01\delta}$  mode has been presented. Coupling ( $\beta$ ), external quality factor ( $Q_{ext}$ ), loaded quality factor ( $Q_L$ ),  $Q_u$  and resonant frequency of DR in MIC environment have been measured. From these measured quantities, the equivalent circuit parameters of DR have been calculated.

Design of a oscillator containing DR as a frequency determining passive element has

Software has been developed to calculate the Q-factor and various losses. This software can be used in the design of microwave circuit containing the DR such as filters, mixer and oscillator.

## 5.2 Suggestion for future development

Following suggestion can be incorporated in any future work.

1. Experimental procedure to measure the coupling between DR and suspended substrate stripline for higher order mode can be developed.
2. Oscillator at higher frequency using DR can be designed.

# Appendix A

## Integral Constant:

The general expressions of  $I_1$  and  $I_2$  are

$$I_1 = \int_0^d r J_1^2(k_r r) dr \quad (\text{A.1})$$

$$I_2 = \int_d^\infty r K_1^2(k_a r) dr \quad (\text{A.2})$$

Where  $J_1$  and  $K_1$  are the Bessels function of first kind zero order and first kind first order respectively. The final expressions of  $I_1$  and  $I_2$  after integration are given by;

$$I_1 = \frac{d^2}{2} [J_1^2(k_r d) - J_0(k_r d) J_2(k_r d)] \quad (\text{A.3})$$

$$I_2 = -\frac{J_0(k_r d)}{K_0(k_a d)} \frac{d^2}{2} [K_1^2(k_a d) - K_0(k_a d) K_2(k_a d)] \quad (\text{A.5})$$

# Bibliography

- [1] S. Maj and J.W.Modelski, "Application of dielectric resonator on microstrip line for a measurement of complex permittivity", in 1984 IEEE MTT-S /SIInt. Microwave Symp. Dig., pp. 525-527.
- [2] Y. Kobayashi, T. Aoki, and Y. Kabe, "Influences of conductor shielding on Q-facyor of  $TE_0$  dielectric resonator", IEEE Trans. Microwave Theory Tech., Vol. MTT-33, pp. 1361-1366, Dec. 1985.
- [3] K.A.Zaki and C.Chen "Loss Mechanism in Dielectric Loaded Resonators" IEEE Trans. Microwave Theory and Technique, Vol.MTT33,pp1448-1452, Dec 1985.
- [4] M.M.Taheri and D.M.Syahkal "Computation of Q-factor of Dielectric Loaded Cylindrical Cavity Resonator", Proc.Inst.Elc.Eng., Vol.137, Pt.H, no.6 pp. 372-376 Dec. 1990.
- [5] D. Kajfej, "Incremental frequency rule for computing the Q-factor of shielded  $TE_{0mp}$  dielectric resonator", IEEE Trans. Microwave Theory and Tech-nique, Vol.MTT32, pp. 941-943, Aug. 1984.
- [6] R.K.Mongia and P.Bhartia "Accurate conductor Q-factar of Dielectric Res-onator placed in MIC environment", IEEE Trans. Microwave Theory and Tech-nique, Vol. MTT41, pp. 445-49, Macch 1993.
- [7] I.Bahl and P.Bhartiya, "Microwave solid state circuit design", Willy Interna-



- [8] E.L. Ginzton, "Microwave Measurements", New York McGraw Hill, pp. 391-427, 1957.
- [9] A.Podcameni et al., "Unloaded quality factor measurement for MIC dielectric resonator application", Elect. Lett. Vol. 17, pp. 656-658, Sept. 1981.
- [10] <sup>P.S</sup> ~~A.P.S~~ Khanna and Y. Garault, "Determination of loaded, unloaded and external quality factors of dielectric resonator coupled to a microstrip line", IEEE Trans. Microwave Theory and Technique Vol.31, pp. 261-264, March 1983.
- [11] R.K.Shukla and A.Biswas "Coupling between off-layered Dielectric Resonators in Suspended Substrate", Microwave and Optical Technology Letters, Vol.11, no.1, Jan 1996.
- [12] R.K.<sup>h</sup>Shukla, " For millimeter wave application", M.Tech thesis I.I.T Kanpur, 1995.
- [13] Y.Kobayashi, T.Aoki and Y.Kabe, "Influence of conductor shielded on the Q-factor of  $TE_0$  Dielectric Resonator", IEEE Trans Microwave Theory and technique Vol. MTT41, pp. 1361-1366, Dec. 1995.
- [14] Trans. Tech, Inc. "Dielectric Resonators", pp22-24, Oct1990.
- [15] Rogers, Selected Guide for Microwave Product.
- [16] D. Kajfej and P. Guillon, "Dielectric Resonators", Artech House, Norwood MA, 1986.
- [17] P.C.L. Yip, "High frequency circuit design and measurement", Chapman and Hall Hong-Kong, 1990.
- [18] K. Imai and H. Nakakita, "A 22-GHz-Band Low-Noise Down-Converter for Satellite Broadcast Receivers", IEEE Trans. Microwave Theory and technique

- [19] G. Gonzalez, "Microwave Transistor Amplifiers Analysis and Design", Printice-Hall Inc., Englwood cliffs. N.J.



122312

## Date Slip

This book **A** to be returned on the  
date last stamped **122312**

date last stamped

# A

**122312**

EE-1996-M-KUM-EXP